



# Resonance of Periodic Combination Antiviral Therapy and Intracellular Delays in Virus Model

Cameron J. Browne<sup>1</sup> · Xuejun Pan<sup>2</sup> · Hongying Shu<sup>3</sup> · Xiang-Sheng Wang<sup>1</sup> 

Received: 9 August 2019 / Accepted: 23 January 2020

© Society for Mathematical Biology 2020

## Abstract

There is a substantial interest in detailed models of viral infection and antiviral drug kinetics in order to optimize the treatment against viruses such as HIV. In this paper, we study within-viral dynamics under general intracellular distributed delays and periodic combination antiviral therapy. The basic reproduction number  $R_0$  is established as a global threshold determining extinction versus persistence, and spectral methods are utilized for analytical and numerical computation of  $R_0$ . We derive the critical maturation delay for virus and optimal phase difference between sinusoidally varying drug efficacies under various intracellular delays. Furthermore, numerical simulations are conducted utilizing realistic pharmacokinetics and gamma-distributed viral production delays for HIV. Our results demonstrate that the relative timing of the key viral replication cycle steps and periodic antiviral treatment schedule involving distinct drugs all can interact to critically affect the overall viral dynamics.

**Keywords** Antiviral therapy · Intracellular delays · Virus model · Basic reproduction number · Spectral analysis

**Mathematics Subject Classification** 92B05 · 37N25

## 1 Introduction

Modeling within-host virus dynamics has been an extensive area of research in mathematical biology. For example, models of HIV dynamics under antiretroviral therapy (ART) have been utilized to gain insight on the kinetics of HIV infection and promising treatment strategies (Adams et al. 2005; Wei et al. 1995; Perelson et al. 1996; Rong

---

✉ Xiang-Sheng Wang  
xswang@louisiana.edu

<sup>1</sup> Department of Mathematics, University of Louisiana at Lafayette, Lafayette, LA 70503, USA

<sup>2</sup> Tongji Zhejiang College, Jiaxing, Zhejiang, China

<sup>3</sup> School of Mathematics and Information Science, Shaanxi Normal University, Xi'an 710062, China

et al. 2007). ART typically consists of a combination of antiviral medications acting at different stages of the viral replication stages. In particular, reverse-transcriptase inhibitors (RTIs) block reverse transcription (RT) after cell infection and before viral production, whereas protease inhibitors (PIs) target the cell's production of viable viral particles. Although ART has been remarkably successful in controlling HIV, ongoing viral replication can persist during therapy, and drug side effects and adherence continue to be issues. Thus, an important motivation for mathematical models is optimization of combination drug therapies acting on distinct phases of the viral replication cycle.

Viral infection is most simply captured by the standard virus model (Perelson and Nelson 1999); a nonlinear system of three ordinary differential equations (ODEs) incorporates target cells, infected cells and free virus particles as the state variables. A more detailed description involves consideration of the replication stages between virus-cell entry and new (mature) viral production by the infected cell. To account for the time lag between viral entry of a target cell and subsequent initiation of viral production from the newly infected cell, known as the *eclipse phase*, Perelson et al. included discrete and distributed delays in the standard model (Nelson and Perelson 2002). Building upon the delay model, many authors consider virus models with age structure in the infected cell compartment where the death (lysis) and viral production rate can vary with age since the infection of the cell (Browne and Pilyugin 2013; Nelson et al. 2004; Rong et al. 2007; Huang et al. 2012).

Given that cell infection and viral production are the fundamental steps in the replication cycle, perhaps the most effective way to incorporate heterogeneity in infected cell processes is to assume that both the eclipse and viral production phases are distributed delays (Shu et al. 2013). Here, we extend previous models by generalizing an age-structured system, with eclipse and virus-producing stages, to an infinite-delay system with probability distributions describing the time taken in each of these stages. In this way, recent experimental estimates of these distributions (Beauchemin et al. 2017) can be accurately quantified in the virus models. Also, the kinetics of distinct classes of drugs can be incorporated in relation to their timing with respect to the key viral replication stages, building upon previous virus models with antiviral therapy (Rong et al. 2007; Wang et al. 2016). In addition, the probability distributions of eclipse and viral production stage are convenient for threshold dynamics analysis in the case of periodic antiviral therapy.

Periodicity in antiviral efficacies occurs as a consequence of the discrete nature of drug intake for patients. The magnitude of fluctuations in antiviral drug efficacy within patients depends upon dosing regimen, adherence and pharmacodynamic properties of the medication (Shen et al. 2008; Vaidya and Rong 2017). Several works have explored the dynamics of virus models with time-varying combination antiviral therapy, treatment optimization with respect to minimizing the reproduction number  $R_0$  and the threshold quantity determining viral extinction versus persistence (De Leenheer 2009; Vaidya and Rong 2017; Wang et al. 2014). The phase difference between distinct antiviral efficacies was found to critically affect  $R_0$  for the standard ODE virus model with periodic drug efficacy functions as small amplitude perturbations from constant level (Browne and Pilyugin 2012), “bang–bang” (Browne and Pilyugin 2016) and more realistic pharmacokinetic functions (Wang and Zhao 2013). Furthermore, Neagu et

al. (2018) argued that inherent delays in the viral replication cycle can substantially affect viral dynamics during periodic (single-drug) antiviral treatment. Here, we further these previous results by rigorous analysis of  $R_0$  and resulting threshold dynamics in a general distributed delay virus model with periodic antiviral drug efficacies. In particular, utilizing the definition of  $R_0$  in the periodic infinite-dimensional setting (Bacaër and Oufki 2007; Bacaër and Abdurahman 2008; Bacaër and Dads 2012; Posny and Wang 2014; Zhao 2017a), we develop analytical and numerical methods to optimize periodic combination therapy for viral infections with a variety of viral intracellular delay distributions. Our results demonstrate that the relative timing of the key viral replication cycle steps, periodic antiviral treatment schedule and phase difference between distinct drugs all can interact to critically affect the overall viral dynamics.

[2]

## 80 2 The Model

81 We begin by considering the following extension of an age-structured virus model  
 82 originally proposed by Nelson et al. (2004):

$$\begin{aligned}
 S'(t) &= \lambda - \delta S(t) - k S(t) V(t), \\
 \left( \frac{\partial}{\partial t} + \frac{\partial}{\partial \tau} \right) j(t, \tau) &= -(\mu_1(\tau) + \gamma(\tau)) j(t, \tau), \quad j(t, 0) = k S(t) V(t), \\
 \left( \frac{\partial}{\partial t} + \frac{\partial}{\partial a} \right) i(t, a) &= -\mu_2(a) i(t, a), \quad i(t, 0) = \int_0^\infty \gamma(\tau) j(t, \tau) d\tau, \\
 V'(t) &= \int_0^\infty q(a) i(t, a) da - dV(t).
 \end{aligned} \tag{1}$$

83 Here,  $S(t)$  is the population size of healthy cells,  $j(t, \tau)$  is the density of infected cells  
 84 in eclipse phase (before viral production begins) with respect to age since cell infection  
 85  $\tau$ ,  $i(t, a)$  is the density of productively infected cell concentration with respect to time  
 86 elapsed since initiation of viral production,  $a$ , and  $V(t)$  is the viral load concentration.  
 87 The healthy cells replenish with constant recruitment rate  $\lambda$  and per capita death rate  
 88  $\delta$ . In the absence of viral infection, the healthy cells will reach at the equilibrium  
 89  $\bar{S} = \lambda/\delta$ . The infection of healthy cells is modeled by a mass action term  $kSV$ , where  
 90  $k$  is the infectivity rate. The death rate of infected cells in the eclipse phase is  $\mu_1(\tau)$ ,  
 91 and the rate at which infected cells transition to viral production stage is  $\gamma(\tau)$ , and  
 92 both depend on time since cell infection  $\tau$ . Additionally,  $\mu_2(a)$  and  $q(a)$  are the age-  
 93 dependent death rate and viral production rate for productively infected cells. System  
 94 (1) directly extends the ordinary differential equation virus model with infected cells  
 95 to be divided into eclipse and virus-producing stages (Buonomo and Vargas-De-León  
 96 2012), by introducing continuous age structures in each class. We are interested in  
 97 a detailed description of the progression of infected cells during typical replication  
 98

cycle; thus, we do not consider the small fraction of infected cells, which are in the resting state, and form the latent reservoir (Rong and Perelson 2009).

Next, we incorporate time-varying combination antiviral treatment into (1):

$$102 \quad S'(t) = \lambda - \delta S(t) - (1 - \eta_1(t))kS(t)V(t), \quad (2)$$

$$103 \quad \left( \frac{\partial}{\partial t} + \frac{\partial}{\partial \tau} \right) j(t, \tau) = -(\mu_1(\tau) + \gamma(\tau))j(t, \tau), \quad j(t, 0) = (1 - \eta_1(t))kS(t)V(t),$$

$$104 \quad \left( \frac{\partial}{\partial t} + \frac{\partial}{\partial a} \right) i(t, a) = -\mu_2(a)i(t, a), \quad i(t, 0) = \int_0^{\infty} \gamma(\tau)j(t, \tau)d\tau,$$

$$105 \quad V'(t) = (1 - \eta_2(t)) \int_0^{\infty} q(a)i(t, a)da - dV(t), \quad (3)$$

107 where  $\eta_1(t)$  and  $\eta_2(t)$  are the efficacies of reverse-transcriptase inhibitors (RTIs) and  
108 protease inhibitors (PIs), respectively. An extension of system (3) with more detailed  
109 model of the action of the RTI is discussed at the end of this section, in Remark 1.

110 We assume that the drug efficacies,  $\eta_1(t)$  and  $\eta_2(t)$ , are at least piecewise continuous  
111 periodic functions with a common period  $T$ , representative of a periodic therapy, and  
112  $\eta_1(t), \eta_2(t) \in [0, 1]$  for all  $t \in \mathbb{R}$ . Two particular examples of periodic drug efficacies  
113 we consider in this paper for explicit analytical and numerical results are:

114 1. *Sinusoidal perturbations from constant efficacy* (Browne and Pilyugin 2012)

$$115 \quad \eta_i(t) = e_i + \varepsilon a_i \cos \omega t, \quad (4)$$

116 where  $e_i$  is the constant (mean) drug efficacy,  $\varepsilon a_i$  is amplitude of small amplitude  
117 oscillation, and  $\omega = 2\pi/T$  with  $T$  being the period of drug administration.

118 2. *Classical dose-response with impulse and exponential decays* (Shen et al. 2008)

$$119 \quad \eta_i(t) = \frac{1}{1 + \left( \frac{\text{IC}_{50i}}{D_i(t)} \right)^{m_i}}, \quad D_i(t) = C_i \left( e^{-r_i(t \bmod T)} + \sum_{n=1}^{\infty} \delta(t - nT) \right), \quad (5)$$

120 where  $D_i(t)$  is the drug concentration in the blood,  $\text{IC}_{50i}$  is the concentration at  
121 50% target inhibition,  $m_i$  is a slope parameter analogous to the Hill coefficient,  
122  $C_i = C_{\max i} / (1 - e^{-r_i T})$  with  $C_{\max i}$  is the maximal concentration achieved in  
123 the blood,  $r_i$  is the decay rate of drug concentration, and  $\delta(t)$  is the Dirac delta  
124 function.

125 The first example, small amplitude sinusoidal drug efficacies, will allow for analytic  
126 approximation of  $R_0$  and also can resemble small variations in antiviral drug effi-  
127 cacy under daily periodic dosing. The second example has been utilized to model  
128 pharmacodynamics of antiviral medications (Vaidya and Rong 2017).

129 The equations in model (3) can be converted to a delay differential equation system.  
 130 By standard application of method of characteristics, we obtain

131  $j(t, \tau) = k(1 - \eta_1(t - \tau))S(t - \tau)V(t - \tau)e^{-\int_0^\tau (\mu_1(s) + \gamma(s))ds},$

132  $i(t, a) = \int_0^\infty \gamma(\tau)\beta(t - a - \tau)S(t - a - \tau)V(t - a - \tau)e^{-\int_0^\tau (\mu_1(s) + \gamma(s))ds}d\tau$   
 133  $e^{-\int_0^a \mu_2(s)ds},$

135 where  $\beta(t) = k(1 - \eta_1(t))$ . Define  $p(t) = 1 - \eta_2(t)$ . Substituting this into the equation  
 136 for  $V'(t)$  yields

137  $V'(t) = p(t) \int_0^\infty \int_0^\infty q(a)\gamma(\tau)\beta(t - a - \tau)S(t - a - \tau)V(t - a - \tau)$   
 138  $e^{-\int_0^\tau (\mu_1(s) + \gamma(s))ds}e^{-\int_0^a \mu_2(s)ds}d\tau da - dV(t). \quad (6)$

140 Equations (2) and (6) together with the initial conditions for viral load  $V(t)$  on  $(-\infty, 0]$   
 141 can formulate a closed system with time delay. Assuming that  $V(-\infty)$  is bounded,  
 142 we rewrite (6) as an integral equation

143  $V(t) = \int_0^\infty e^{-ds} p(t - s) \int_0^\infty \int_0^\infty q(a)\gamma(\tau)\beta(t - s - a - \tau)$   
 144  $S(t - s - a - \tau)V(t - s - a - \tau)$   
 145  $e^{-\int_0^\tau (\mu_1(s) + \gamma(s))ds}e^{-\int_0^a \mu_2(s)ds}d\tau dads. \quad (7)$

147 We now seek to extend the viral model by allowing more general distributed delays  
 148 with respect to the key stages in the viral replication cycle. Several previous works  
 149 (Culshaw and Ruan 2000) have assumed there is a fixed intracellular delay  $\tau_0$ , so  
 150 that  $\gamma(\tau) = \delta(\tau - \tau_0)$  where  $\delta(\tau)$  is the Dirac delta function. Others have assumed  
 151 an exponentially distributed eclipse phase, in particular the extended classical virus  
 152 ODE model with additional eclipse (or latent) infection compartment (Buonomo and  
 153 Vargas-De-León 2012). A more general approach that has been studied is to consider  
 154 a distributed delay according to a kernel, which we denote here by  $\pi(\tau)$ , describing  
 155 the probability density function for the age  $\tau$  that a (surviving) infected cell becomes  
 156 productive (Shu et al. 2013). If  $P(\tau)$  is the survival rate during the eclipse phase,  
 157 then  $\theta := \int_0^\infty P(\tau)\pi(\tau)d\tau$  is the probability of an infected cell becoming produc-  
 158 tive and  $f(\tau) = (P(\tau)\pi(\tau))/\theta$  is the conditional probability density for the age  
 159  $\tau$  that a cell becomes productive. Note that this description of the eclipse phase  
 160 generalizes the age-structured model which considers the exponential distributions  
 161  $\pi(\tau) = \gamma(\tau)e^{-\int_0^\tau \gamma(s)ds}$  and  $P(\tau) = e^{-\int_0^\tau \mu_1(s)ds}$ . Similarly, we can generalize the

productively infected cell kinetics by assuming an arbitrary survival probability distribution  $\sigma(a)$  with  $g(a) = (q(a)\sigma(a))/N$  corresponding to the conditional probability of producing infectious virus arising  $a$  units of time after the cell becomes productively infected where  $N = \int_0^\infty q(a)\sigma(a)da$  is the burst size (average # of virus produced during infected cell life). For the age-structured model (3), we choose  $\sigma(a) = e^{-\int_0^a \mu_2(s)ds}$ . With these features in mind, we extend the delay differential system (2)–(6) as

$$S'(t) = \lambda - \delta S(t) - \beta(t)S(t)V(t), \quad (8)$$

$$V'(t) = \theta N p(t) \int_0^\infty \int_0^\infty g(a)f(\tau)\beta(t-a-\tau)S(t-a-\tau)V(t-a-\tau)d\tau da - dV(t). \quad (9)$$

The integral equation (7) can then be generalized by writing (9) as follows:

$$V(t) = \theta N \int_0^\infty \int_0^\infty \int_0^\infty e^{-ds} p(t-s)g(a)f(\tau) \beta(t-s-a-\tau)S(t-s-a-\tau)V(t-s-a-\tau)d\tau dads. \quad (10)$$

It is obvious that any PDE in the age-structured model can be converted into the above DDE by setting

$$\theta = \int_0^\infty \gamma(\tau)e^{-\int_0^\tau [\gamma(s)+\mu_1(s)]ds} d\tau, \quad f(\tau) = \frac{1}{\theta} \gamma(\tau)e^{-\int_0^\tau [\gamma(s)+\mu_1(s)]ds},$$

$$N = \int_0^\infty q(a)e^{-\int_0^a \mu_2(s)ds} da, \quad g(a) = \frac{1}{N} q(a)e^{-\int_0^a \mu_2(s)ds}.$$

However, the above relation is not necessarily invertible in the sense that any DDE (8), (9) can be converted into the PDE with age structure. Besides being more general, the DDE formulation in terms of probability distributions,  $f(\tau)$  and  $g(a)$ , has also advantages in the spectral analysis to come in this paper. Furthermore, from a biological point of view, it is convenient to formulate the kinetics of the main phases of the infected cell cycle as distributions which can be matched to experimental data.

Another generalization of model (1) was proposed in Wang and Dong (2018). Our model differs from that in Wang and Dong (2018) in the sense that we incorporate periodic antiviral treatment and our model system is nonautonomous. In general, it is a challenge to compute the basic reproduction number and study the model dynamics for periodic systems with time delays.

191 The dynamics of (8), (9) (equivalently (10)) will be analyzed in what follows;  
 192 however, we also remark here that the system can be extended with respect to modeling  
 193 reverse transcription (RT) in infected cells as described below.

194 **Remark 1** A more detailed description of antiviral action with respect to infected cell  
 195 life can take into account that RT inhibitors act during the eclipse phase interfering  
 196 with RT transcriptase, a necessary step for viral replication. In “Appendix A”, we  
 197 extend the age-structured model by adding an extra compartment explicitly tracking  
 198 the process of RT during the eclipse phase of infected cell. In the special case that  
 199 RT occurs at a fixed time,  $r$ , after viral entry, then the delay differential equation for  
 200 the virus,  $V(t)$ , reduces to (9) with  $\beta(t)$  shifted by  $r$  units of time, i.e.,  $\beta(t+r)$ .  
 201 In particular, all of the formulae we will derive in Sect. 4.2 concerning reproduction  
 202 number dependent on the periodic forcing hold in the extended model with the RT  
 203 delay  $r$  shifting the effective infection rate as  $\beta(t+r)$ .

### 204 3 Threshold Analysis of Model

#### 205 3.1 Boundedness

206 Throughout this paper, we assume that  $g(a)$  and  $f(\tau)$  are probability density functions  
 207 on  $\mathbb{R}_+$  with exponentially decay rate at infinity.

208 (H) *There exists  $\alpha_0 > 0$  such that both  $g(t)e^{\alpha_0 t} \rightarrow 0$  and  $f(t)e^{\alpha_0 t} \rightarrow 0$  as  $t \rightarrow \infty$ .*

209 To study the model system with the infinite delay, we first introduce the weighted  
 210 continuous function space. For a given  $\alpha \in (0, \alpha_0)$ , we define  $C_\alpha$  to be the subspace  
 211 of  $C(\mathbb{R}_-, \mathbb{R})$  such that  $\phi(\theta)e^{\alpha\theta}$  is uniformly continuous on  $\mathbb{R}_- = (-\infty, 0]$  and the  
 212 norm

$$213 \|\phi\|_\alpha := \sup_{\theta \in \mathbb{R}_-} |\phi(\theta)e^{\alpha\theta}|$$

214 is finite. It is easily seen that  $C_\alpha$  is a Banach space equipped with the norm  $\|\cdot\|_\alpha$ , and  
 215 system (8), (9) is well-posed in  $C_\alpha \times C_\alpha$ .

216 Let  $C_\alpha^+$  be the nonnegative cone collecting all nonnegative functions in  $C_\alpha$ . We  
 217 intend to show that if the initial profile is contained in the  $C_\alpha^+ \times C_\alpha^+$ , so is the solution  
 218 for any  $t > 0$ . It can be proved by contradiction that  $S(t) \geq 0$ . If  $t_0 \geq 0$  is the infimum  
 219 of all  $t$  with  $S(t) < 0$ , then  $S(t_0) = 0$  and  $S'(t_0) \leq 0$ , which obviously contradict Eq.  
 220 (8). Actually, we have  $S(t) > 0$  for all  $t > 0$ . Next, we integrate (9) to obtain

$$221 \quad V(t) = e^{-dt} V(0) + \theta N \int_0^t \int_0^\infty \int_0^\infty e^{-d(t-s)} p(s) g(a) f(\tau) \\ 222 \quad \beta(s-a-\tau) S(s-a-\tau) V(s-a-\tau) dt d\tau da ds,$$

224 from which nonnegativity of  $V(t)$  follows. If, further,  $V(0) > 0$ , it is easy to show  
 225 that  $V(t) > 0$  for all  $t > 0$ .

We also want to show that the solution of the model system with nonnegative initial conditions is bounded above. From (8), we have  $S'(t) \leq \lambda - \delta S(t)$ . By comparison principle, we obtain  $\limsup_{t \rightarrow \infty} S(t) \leq \lambda/\delta$ . Furthermore, if  $S(t) \leq \lambda/\delta$  for some  $t = t_0$ , then  $S(t) \leq \lambda/\delta$  for all  $t \geq t_0$ . Define an auxiliary function

$$U(t) = \theta N \int_t^\infty \int_0^\infty \int_0^\infty e^{-d(t-s)} p(s) g(a) f(\tau) \beta(s-a-\tau) S(s-a-\tau) V(s-a-\tau) da d\tau ds.$$

It is readily seen that  $U(t) \geq 0$  for all  $t \geq 0$ , and

$$U'(t) = -\theta N p(t) \int_0^\infty \int_0^\infty g(a) f(\tau) \beta(t-a-\tau) S(t-a-\tau) V(t-a-\tau) da d\tau - dU(t).$$

Add this equation to (8) and (9) yields

$$S'(t) + U'(t) + V'(t) = \lambda - \delta S(t) - \beta(t) S(t) V(t) - dU(t) - dV(t).$$

By comparison principle, we have  $\limsup_{t \rightarrow \infty} [S(t) + U(t) + V(t)] \leq \lambda / \min\{\delta, d\}$ .

Note that system (8), (9) is a nonautonomous with a periodic solution semiflow  $U(t, s)$  on  $C_\alpha \times C_\alpha$  satisfying  $U(t, t) = I$ ,  $U(t, s)U(s, r) = U(t, r)$  and  $U(t + T, s + T) = U(t, s)$ . To construct an equivalent autonomous semigroup, we use the idea in Saperstone (1981) (see also Rebelo et al. 2014; Zhao and Hutson 1994) to introduce the compact metric space

$$\mathbb{R}_T := \mathbb{R}/T\mathbb{Z} = \{r \in \mathbb{R} : r_1 \sim r_2 \Leftrightarrow (r_1 - r_2)/T \in \mathbb{Z}\}$$

equipped with the distance  $d(r_1, r_2) = |e^{2i\pi r_1/T} - e^{2i\pi r_2/T}|$ . Define a semigroup  $\Psi(t)$  on  $X = C_\alpha \times C_\alpha \times \mathbb{R}_T$  as

$$\Psi(t)(\phi, r) = (U(t+r, r)\phi, t+r), \quad \phi = (u, v) \in C_\alpha \times C_\alpha, \quad r \in \mathbb{R}_T.$$

$\Psi(t)$  is well-defined since

$$\begin{aligned} \Psi(t)(\phi, r+T) &= (U(t+r+T, r+T)\phi, t+r+T) = (U(t+r, r)\phi, t+r) \\ &= \Psi(t)(\phi, r). \end{aligned}$$

It is also easy to verify that  $\Psi(0) = I$  and

$$\begin{aligned} \Psi(t)\Psi(s)(\phi, r) &= (U(t+s+r, s+r)U(s+r, r)\phi, t+s+r) \\ &= (U(t+s+r, r)\phi, t+s+r) = \Psi(t+s)(\phi, r). \end{aligned}$$

The argument in the preceding paragraph indicates that  $\Psi(t)$  is point dissipative. Moreover, for any constant  $C > \lambda / \min\{\delta, d\}$ , the bounded region  $\Gamma_C := \{(u, v, r) \in$

255  $X : \|u\|_\alpha \leq C, \|v\|_\alpha \leq C\}$  is absorbing in the sense that it contains all possible  
 256 attractors of  $\Psi(t)$ .

257 Finally, we show that the set of trajectories  $\gamma^+(\Gamma_C) = \bigcup_{\phi \in \Gamma_C} \gamma^+(\phi)$  is also  
 258 bounded. To see this, we consider the auxiliary system with (8) replaced with

259 
$$S'(t) = \lambda - \delta S(t). \quad (11)$$

260 The differential equation for  $V(t)$  is still (9). Any initial condition  $(\phi, r)$  in  $\Gamma_C$  is  
 261 bounded by  $(S_0, V_0, r)$  with  $S_0(\theta) = V_0(\theta) = Ce^{-\alpha\theta}$  for  $\theta \in \mathbb{R}_+$ . Thus, by compar-  
 262 ison principle,  $U(t, r)\phi \leq U(t, r)(S_0, V_0)$ . We can use a similar argument as in the  
 263 proof of point dissipativeness of  $\Psi(t)$  to find a constant  $\bar{C} > 0$  (which depends on  $C$ )  
 264 such that  $\gamma^+(\Gamma_C) \subset \Gamma_{\bar{C}}$ .

265 **3.2 Basic Reproduction Number**

266 Following Bacaër and Ouifki (2007), Bacaër and Abdurahman (2008), Bacaër and  
 267 Dads (2012), Zhao (2017a), we can define the reproduction number for the renewal  
 268 type Eq. (10) as the spectral radius of the next-generation operator,  $R_0 = \rho(L)$ , where

$$(L\phi)(t) = \theta N \bar{S} \int_0^\infty \int_0^\infty \int_0^\infty e^{-ds} p(t-s) g(a) f(\tau) \beta(t-s-a-\tau) \phi(t-s-a-\tau) d\tau da ds, \quad (12)$$

269 acting on the space of continuous  $T$ -periodic functions on  $\mathbb{R}$ , denoted as  $\mathbb{P}_T$ . For any  
 270 infinite sequence of continuous and uniformly bounded  $\phi_n \in \mathbb{P}_T$ , we can show that  
 271 both  $L\phi_n$  and  $(L\phi_n)'$  are uniformly bounded (since  $g$ ,  $f$  are probability distributions  
 272 and  $\beta(t)$ ,  $p(t)$  are periodic functions). By the Arzela–Ascoli theorem,  $L$  is a compact  
 273 operator on  $\mathbb{P}_T$ . Obviously,  $L$  is a positive operator on the cone of nonnegative functions  
 274 in  $\mathbb{P}_T$ . If  $p(t) > 0$  and  $\beta(t) > 0$  for all  $t \in \mathbb{R}$ , then  $L$  is strongly positive and Krein–  
 275 Rutman theorem (Du 2006, Theorem 1.2) implies that  $R_0 = \rho(L)$  is an eigenvalue of  
 276 the operator  $L$  with a corresponding positive eigenfunction  $u(t)$ ; that is,

$$R_0 u(t) = \theta N \bar{S} \int_0^\infty \int_0^\infty \int_0^\infty e^{-ds} p(t-s) g(a) f(\tau) \beta(t-s-a-\tau) u(t-s-a-\tau) d\tau da ds. \quad (13)$$

278 Observe that the definition of  $R_0$  in (13) involves an eigenvalue equation for an infinite-  
 279 dimensional operator. In Sect. 15, we investigate a formulation of  $R_0$  amenable to  
 280 analytical methods, and we will develop different numerical methods to compute  $R_0$   
 281 in Sect. 4.3.



### 283 3.3 Extinction and Persistence of Infection

284 In the following theorem, we state that the basic reproduction number is the threshold  
 285 parameter for the model dynamics. First, we demonstrate that if  $R_0 < 1$ , then the  
 286 disease-free equilibrium  $E_0 = \{\bar{S}, 0\}$  with  $\bar{S} = \lambda/\delta$  is globally attractive in  $X$ .

287 **Theorem 2** *Assume (H). If  $R_0 < 1$ , there exists  $\alpha_1 \in (0, \alpha_0)$  such that, for any  $\alpha \in$*   
 288  *$(0, \alpha_1)$ , the disease-free equilibrium  $E_0 = \{\bar{S}, 0\}$  is globally attractive in  $C_\alpha^+ \times C_\alpha^+$ .*

289 **Proof** Recall that  $\mathbb{P}_T$  is the Banach space of continuous  $T$ -periodic functions on  $\mathbb{R}$   
 290 equipped with the supremum norm. We introduce the following parametrized compact  
 291 operator on  $\mathbb{P}_T$ :

$$292 \quad (L_\mu \phi)(t) = \theta N \bar{S} \int_0^\infty \int_0^\infty \int_0^\infty e^{\mu(s+a+\tau)-ds} p(t-s)g(a)f(\tau) \\ \beta(t-s-a-\tau)\phi(t-s-a-\tau)d\tau dads, \quad (14)$$

294 for all real  $\mu < \min\{d, \alpha_0\}$ . Obviously,  $\rho(L_0) = \rho(L) = R_0 < 1$ ; see (12). More-  
 295 over,  $\rho(L_\mu)$  is continuous (Degla 2008, Theorem 2.1) and increasing (Burlando 1991,  
 296 Theorem 1.1) in  $\mu$ . Hence, there exists a small  $\nu > 0$  such that  $\rho(L_\nu) < 1$ . Krein-  
 297 Rutman theorem implies that the principal eigenfunction  $\phi \in \mathbb{P}_T$  is positive. Let  
 298  $\varepsilon = \bar{S}/\rho(L_\nu) - \bar{S} > 0$  and  $v(t) = e^{-\nu t}\phi(t)$ . It follows that

$$299 \quad v(t) = \theta N(\bar{S} + \varepsilon) \int_0^\infty \int_0^\infty \int_0^\infty e^{-ds} p(t-s)g(a)f(\tau)\beta(t-s-a-\tau) \\ 300 \quad v(t-s-a-\tau)d\tau dads.$$

301 Differentiating both sides gives a periodic renewal equation

$$302 \quad v'(t) = -dv(t) + \theta N(\bar{S} + \varepsilon)p(t) \int_0^\infty \int_0^\infty \beta(t-a-\tau)g(a)f(\tau)v(t-a-\tau)dad\tau.$$

304 The above equation is also a perturbation of the linearization of (7). Now, we choose  
 305  $\alpha_1 = \min\{\nu/2, \alpha_0/2\}$  and let  $\{S(t), V(t)\}$  be any solution of (8), (9) with the initial  
 306 condition in  $C_\alpha \times C_\alpha$ , where  $\alpha \in (0, \alpha_1)$ . Since  $\limsup_{t \rightarrow \infty} S(t) \leq \bar{S}$ , there exists  
 307  $t_0 > 0$  such that  $S(t) < \bar{S} + \varepsilon$  for all  $t > t_0$ . In view of  $2\alpha < \nu$ , the functions  $V(t)e^{\nu t}$   
 308 and  $S(t)V(t)e^{\nu t}$  are uniformly bounded for all  $t \in \mathbb{R}_-$ . Consequently, there exists  
 309  $C > 0$  such that  $Cv(t) \geq V(t)$  and  $(\bar{S} + \varepsilon)Cv(t) \geq S(t)V(t)$  for all  $t \leq t_0$ . Denote

$$310 \quad F(t) = \theta N(\bar{S} + \varepsilon)p(t) \iint_{\tau+a \geq t-t_0} \beta(t-a-\tau)g(a)f(\tau)Cv(t-a-\tau)dad\tau.$$

311 It is easily seen that

$$312 Cv'(t) = -dCv(t) + \theta N(\bar{S} + \varepsilon)p(t) \iint_{\tau+a \leq t-t_0} \beta(t-a-\tau)g(a) \\ 313 f(\tau)Cv(t-a-\tau)dad\tau + F(t),$$

314 for  $t \geq t_0$ . On the other hand, from the choice of  $C$  we have

$$315 V'(t) \leq -dV(t) + \theta N(\bar{S} + \varepsilon)p(t) \iint_{\tau+a \leq t-t_0} \beta(t-a-\tau)g(a)f(\tau) \\ 316 V(t-a-\tau)dad\tau + F(t)$$

317 for all  $t \geq t_0$ . By comparison principle,  $Cv(t) \geq V(t)$  for all  $t \geq t_0$ . Especially,  
318  $V(t) \rightarrow 0$  as  $t \rightarrow \infty$ . It then follows from (8) that  $S(t) \rightarrow \bar{S}$  as  $t \rightarrow \infty$ .  $\square$

319 **Remark 3** Since the delay is not finite, the Poincaré map for the linearization of (7)  
320 may not be compact on  $C_\alpha$ . Thus, one cannot use a similar argument as in the proof  
321 of Xu and Zhao (2005), Proposition 2.1, to find an upper solution which converges to  
322 zero as  $t$  approaches infinity.

323 When  $R_0 > 1$ , we prove in “Appendix” the following theorem stating that system  
324 (8), (9) is uniformly persistent.

325 **Theorem 4** *Assume (H) and  $\alpha \in (0, \alpha_0)$ . If  $R_0 > 1$ , then there exists  $\delta_0 > 0$  such  
326 that for any initial condition  $(u_0, v_0) \in C_\alpha \times C_\alpha$  with  $v_0(0) > 0$ , the solution  $(S, V)$   
327 of (8), (9) satisfies  $\liminf_{t \rightarrow \infty} S(t) > \delta_0$  and  $\liminf_{t \rightarrow \infty} V(t) > \delta_0$ .*

## 328 4 Computing $R_0$

### 329 4.1 Fourier Analysis

330 In a similar spirit to Bacaër (2007), we consider Fourier expansions of the  $T$ –periodic  
331 functions  $u(t)$ ,  $p(t)$  and  $\beta(t)$ :

$$332 u(t) = \sum_{j \in \mathbb{Z}} c_j e^{ij\omega t}, \quad \frac{\beta(t)}{\langle \beta \rangle} = \sum_{j \in \mathbb{Z}} \beta_j e^{ij\omega t}, \quad \frac{p(t)}{\langle p \rangle} = \sum_{j \in \mathbb{Z}} p_j e^{ij\omega t}, \quad (15)$$

333 where  $\omega = \frac{2\pi}{T}$ ,  $\langle \beta \rangle := \frac{1}{T} \int_0^T \beta(t) dt$  and  $\langle p \rangle := \frac{1}{T} \int_0^T p(t) dt$ . The eigenfunction  $u(t)$   
334 can also be normalized so that  $c_0 = \langle c \rangle = 1$ . Substituting (15) into (13), the eigenvalue

335 equation expands as follows:

$$\begin{aligned}
 336 \quad & \frac{R_0}{\theta N \bar{S} \langle \beta \rangle \langle p \rangle} \sum_{j \in \mathbb{Z}} c_j e^{ij\omega t} = \sum_{m \in \mathbb{Z}} \sum_{l \in \mathbb{Z}} \sum_{n \in \mathbb{Z}} \beta_l p_m c_n e^{i(m+l+n)\omega t} \int_0^\infty e^{-ds} e^{-i(m+n+l)\omega s} ds \\
 337 \quad & \int_0^\infty g(a) e^{-i(l+n)\omega a} da \int_0^\infty f(\tau) e^{-i(l+n)\omega \tau} d\tau \\
 338 \quad & = \sum_{j \in \mathbb{Z}} \sum_{k \in \mathbb{Z}} \sum_{n \in \mathbb{Z}} \beta_{k-n} p_{j-k} c_n e^{ij\omega t} \frac{F_k}{d + ij\omega},
 \end{aligned}$$

339

340 341 where in the last step we make changes of indices  $j = l + m + n$  and  $k = l + n$ . and

$$342 \quad F_k := \int_0^\infty g(a) e^{-ik\omega a} da \int_0^\infty f(\tau) e^{-ik\omega \tau} d\tau. \quad (16)$$

343 We denote

$$344 \quad \gamma = \frac{d}{\theta N \bar{S} \langle \beta \rangle \langle p \rangle}, \quad H_j = \frac{d}{d + ij\omega}. \quad (17)$$

345 346 It is readily seen that

$$347 \quad \gamma R_0 c_j = H_j \sum_{k \in \mathbb{Z}} \sum_{n \in \mathbb{Z}} F_k \beta_{k-n} p_{j-k} c_n. \quad (18)$$

348 349 Note that  $F_k$  is the product of characteristic functions corresponding to probability  
 350 distributions  $g$  and  $f$  evaluated at  $-k\omega$  and  $H_j$  is the characteristic function of the  
 351 exponential distribution evaluated at  $-j\omega$ . Also, recall the product of characteristic  
 352 functions is equal to the characteristic function of sum of independent random  
 353 variables with corresponding probability distributions. Thus, coefficients determining  
 354 the effect of periodicity on reproduction number are influenced by how the periodic  
 355 drug efficacies interact with the probability kernels describing delays in the replication  
 356 cycle.

## 357 4.2 Perturbation Analysis

358 Next, we consider the particular case where the drug efficacies are sinusoidal pertur-  
 359 bations from constant values,  $e_i$ , given by  $\eta_i(t)$  in (4), along with a possible phase  
 360 difference between the distinct drug administrations. Then, it suffices to let

$$361 \quad \frac{\beta(t)}{\langle \beta \rangle} = 1 + 2\varepsilon\alpha_1 \cos \omega t, \quad \frac{p(t)}{\langle p \rangle} = 1 + 2\varepsilon\alpha_2 \cos[\omega(t - \phi)], \quad (19)$$

362 363 where  $\alpha_i = -\frac{a_i}{2(1-e_i)}$ , and  $\phi \in [0, T)$  represents the phase difference between the  
 364 distinct antiviral drug efficacies, i.e.,  $\phi = (\phi_2 - \phi_1) \bmod T$ , where  $\phi_1$  and  $\phi_2$  are

364 the phases of two drug administrations. The phase difference inherently describes the  
 365 timing between dosages of the two drugs in the periodic schedule. It follows that the  
 366 Fourier coefficients for  $\beta(t)$  and  $p(t)$  are as follows:

367  $\beta_0 = p_0 = 1, \quad \beta_1 = \beta_{-1} = \varepsilon\alpha_1, \quad p_1 = \varepsilon\alpha_2 e^{-i\omega\phi}, \quad p_{-1} = \varepsilon\alpha_2 e^{i\omega\phi},$

368 and  $\beta_j = p_j = 0$  for  $|j| \geq 2$ .

369 We assume  $\varepsilon > 0$  is small and write  $\gamma R_0$  and  $c_j$  as power series expansions in  $\varepsilon$ :

370  $\gamma R_0 = \sum_{k \geq 0} \rho_{0k} \varepsilon^k, \quad c_j = \sum_{k \geq 0} c_{jk} \varepsilon^k.$

371 Since  $\beta_j = p_j = 0$  for  $|j| \geq 2$ , we can simply write Eq. (18) as

372 
$$\begin{aligned} \gamma R_0 c_j &= H_j [p_{-1} F_{j+1} (\beta_{-1} c_{j+2} + \beta_0 c_{j+1} + \beta_1 c_j) \\ 373 &\quad + p_0 F_j (\beta_{-1} c_{j+1} + \beta_0 c_j + \beta_1 c_{j-1}) \\ 375 &\quad + p_1 F_{j-1} (\beta_{-1} c_j + \beta_0 c_{j-1} + \beta_1 c_{j-2})] \end{aligned} \quad (20)$$

376 By substituting these expansions into (20) and comparing the coefficients of  $\varepsilon^k$  (with  
 377  $k = 0, 1, 2, 3$ ) on both sides, we obtain

378  $\rho_{00} c_{j0} = H_j F_j c_{j0},$   
 379  $\rho_{01} c_{j0} + \rho_{00} c_{j1} = H_j [F_{j+1} \alpha_2 e^{i\omega\phi} c_{j+1,0} + F_j (\alpha_1 c_{j+1,0} + c_{j1} + \alpha_1 c_{j-1,0})$   
 380  $\quad + F_{j-1} \alpha_2 e^{-i\omega\phi} c_{j-1,0}],$   
 381  $\rho_{02} c_{j0} + \rho_{01} c_{j1} + \rho_{00} c_{j2} = H_j [F_{j+1} \alpha_2 e^{i\omega\phi} (\alpha_1 c_{j+2,0} + c_{j+1,1} + \alpha_1 c_{j0})$   
 382  $\quad + F_j (\alpha_1 c_{j+1,1} + c_{j2} + \alpha_1 c_{j-1,1}) + F_{j-1} \alpha_2 e^{-i\omega\phi} (\alpha_1 c_{j0} + c_{j-1,1} + \alpha_1 c_{j-2,0})],$   
 383  $\rho_{03} c_{j0} + \rho_{02} c_{j1} + \rho_{01} c_{j2} + \rho_{00} c_{j3} = H_j [F_{j+1} \alpha_2 e^{i\omega\phi} (\alpha_1 c_{j+2,1} + c_{j+1,2} + \alpha_1 c_{j1})$   
 384  $\quad + F_j (\alpha_1 c_{j+1,2} + c_{j3} + \alpha_1 c_{j-1,2}) + F_{j-1} \alpha_2 e^{-i\omega\phi} (\alpha_1 c_{j1} + c_{j-1,2} + \alpha_1 c_{j-2,1})].$

386 From the normalization condition  $c_0 = 1$ , we have  $c_{00} = 1$  and  $c_{0k} = 0$  for  $k \geq 1$ . It  
 387 then follows from the first equation (with  $j = 0, \pm 1, \pm 2, \dots$ ) that  $\rho_{00} = H_0 F_0 = 1$   
 388 and  $c_{j0} = 0$  for  $|j| \geq 1$ . Substituting these into the second equation (with  $j = 0, \pm 1$ )  
 389 yields  $\rho_{01} = 0$  and

390  $c_{11} = H_1 F_1 c_{11} + H_1 F_1 \alpha_1 + H_1 \alpha_2 e^{-i\omega\phi},$   
 391  $c_{-1,1} = H_{-1} \alpha_2 e^{i\omega\phi} + H_{-1} F_{-1} \alpha_1 + H_{-1} F_{-1} c_{-1,1}. \quad (21)$

393 It is easy to obtain from the second equation that  $c_{j1} = 0$  for  $|j| \geq 2$ . Next, we set  
 394  $j = 0$  in the third equation to find

395  $\rho_{02} = \alpha_2 F_1 e^{i\omega\phi} (c_{11} + \alpha_1) + \alpha_1 c_{11} + \alpha_1 c_{-1,1} + \alpha_2 F_{-1} e^{-i\omega\phi} (\alpha_1 + c_{-1,1})$   
 396  $= \alpha_1 \alpha_2 (F_1 e^{i\omega\phi} + F_{-1} e^{-i\omega\phi}) + c_{11} (\alpha_2 F_1 e^{i\omega\phi} + \alpha_1) + c_{-1,1} (\alpha_2 F_{-1} e^{-i\omega\phi} + \alpha_1)$

398 Note that  $H_1$  and  $H_{-1}$ , and  $F_1$  and  $F_{-1}$  defined in (17) are conjugates. Thus, on account  
 399 of (21), we obtain

400 
$$\rho_{02} = 2\alpha_1\alpha_2 f_1 + 2(\alpha_1^2 + \alpha_2^2) f_2, \quad (22)$$

402 where

403 
$$f_1 = \operatorname{Re} \frac{F_1 e^{i\omega\phi} + H_1 e^{-i\omega\phi}}{1 - H_1 F_1} = \frac{A \cos(\omega\phi) + B \sin(\omega\phi)}{|1 - H_1 F_1|^2},$$
  
 404 
$$f_2 = \operatorname{Re} \frac{H_1 F_1}{1 - H_1 F_1} = \frac{\operatorname{Re}(H_1 F_1) - |H_1 F_1|^2}{|1 - H_1 F_1|^2}.$$
  
 405

406 Here, we recall that  $H_1 = \frac{d}{d + i\omega}$  and  $F_1 = \int_0^\infty g(a) e^{-i\omega a} da \int_0^\infty f(\tau) e^{-i\omega\tau} d\tau$ , and,  
 407 for simplicity, we have denoted

408 
$$A = (1 - |H_1|^2) \operatorname{Re}(F_1) + (1 - |F_1|^2) \operatorname{Re}(H_1),$$
  
 409 
$$B = -(1 - |H_1|^2) \operatorname{Im}(F_1) + (1 - |F_1|^2) \operatorname{Im}(H_1).$$

411 By choosing  $j = \pm 1$  in the third equation, we further obtain  $c_{12} = c_{-1,2} = 0$ . Finally,  
 412 it is easy to calculate from the fourth equation with  $j = 0$  that  $\rho_{03} = 0$ .

413 We summarize the above calculation in the following theorem displaying the effect  
 414 of sinusoidal drug efficacy perturbations on  $R_0$ , along with the optimal phase difference  
 415  $\phi^*$  between the two drugs.

416 **Theorem 5** *If  $\beta(t)$  and  $p(t)$  are small perturbations of constants as given in (19), then  
 417 the basic reproduction number has the asymptotic formula*

418 
$$R_0 = \frac{\theta N \bar{S} \langle \beta \rangle \langle p \rangle}{d} (1 + \rho_{02} \varepsilon^2 + O(\varepsilon^4)),$$

419 where  $\rho_{02}$  is given as in (22). Furthermore,  $\rho_{02}$  is minimized at the phase difference

420 
$$\phi^* = \frac{T}{2} + \frac{T}{2\pi} \arctan \frac{B}{A} \quad \text{mod } T$$

421 if  $A \geq 0$ , and

422 
$$\phi^* = \frac{T}{2\pi} \arctan \frac{B}{A} \quad \text{mod } T$$

423 if  $A < 0$ .

424 Note that  $\rho_{02}$  is the first coefficient in the expansion of  $R_0$  corresponding to amplitude,  
 425  $\epsilon$ , and therefore will control the effect of periodic perturbations on  $R_0$ . In  
 426 particular, we are interested in the optimal phase difference  $\phi^*$  which will minimize  
 427  $\rho_{02}$  and, in turn, minimize  $R_0$ .

#### 4.3 Numerical Computation

428 We first use finite difference method (Posny and Wang 2014) to compute  $R_0$ , which  
 429 is the principal eigenvalue of the linear operator  $L$  in (12). By defining

431 
$$K(t, s) = \theta N \bar{S} e^{-ds} \beta(t - s) \iint_{a+\tau \leq s} e^{d(a+\tau)} g(a) f(\tau) p(t - s + a + \tau) da d\tau, \quad (23)$$

432 we can rewrite (12) as  $(L\phi)(t) = \int_0^\infty K(t, s)\phi(t - s) ds$ . Given a large integer  $M > 0$ ,  
 433 we discretize the period  $[0, T]$  as  $t_0 \leq t_1 \leq \dots \leq t_M$ , where  $t_j = j\Delta t$  with  $\Delta t = T/M$ .  
 434 For  $j > M$  or  $j < 0$ , we still denote  $t_j = j\Delta t$ . The above linear operator can be  
 435 approximated by a matrix of dimension  $n$ :  $(\hat{L}\hat{\phi})_j = \sum_{k=1}^M \hat{L}_{jk} \hat{\phi}_k$ , where  $\hat{\phi}$  is the  
 436 numerical approximation of  $\phi(x)$  and

437 
$$\hat{L}_{jk} = \Delta t \sum_{l=0}^{\infty} K(t_j, t_{j-k+lM}). \quad (24)$$

438 Here, for convenience, we set  $K(t, s) = 0$  if  $s < 0$ . The kernel  $K(t_j, t_m)$  in (23) can  
 439 be approximated via a standard quadrature formula:

440 
$$K(t_j, t_m) \approx \theta N \bar{S} e^{-dt_m} \beta(t_{j-m}) \Delta t^2 \sum_{k+l \leq m} w_{kl}(m) e^{dt_{k+l}} g(t_k) f(t_l) p(t_{j-m+k+l}),$$

441 where the quadrature weights can be chosen as  $w_{kl}(m) = 1$  and  $w_{0l}(m) = w_{k0}(m) =$   
 442  $w_{kk}(m) = 1/2$  for  $0 < k, l < m$ ; and  $w_{00}(m) = w_{m0}(m) = w_{m0}(m) = 1/6$ . To save  
 443 the computation cost, we use the following recurrence relation to calculate the kernel  
 444 function:

445 
$$K(t_j, t_m) = e^{-d\Delta t} K(t_{j-1}, t_{m-1}) + \theta N \bar{S} e^{-dt_m} \beta(t_{j-m})$$
  
 446 
$$\iint_{t_{m-1} \leq a+\tau \leq t_m} e^{d(a+\tau)} g(a) f(\tau) p(t_{m-1} + a + \tau) da d\tau,$$

447 where the double integral on the right-hand side can be approximated via a standard  
 448 quadrature formula. If the probability density functions  $g$  and  $f$  decay rapidly at  
 449 infinity, the kernel function  $K(t, s)$  in (23) also decays rapidly as  $s \rightarrow \infty$ , and we  
 450 can truncate the series in (24) as a finite sum, say, at  $l_m$ . In our simulation, we choose  
 451  $l_m = 5$  and do not observe significant differences in the results with larger  $l_m$ .

452 Another numerical method in the computation of  $R_0$  is based on the Fourier trans-  
 453 form of periodic functions and spectral decomposition of linear operator  $L$  in (12).  
 454 Let  $M > 0$  be a large even integer. Set  $\Delta t = T/M$  and  $t_j = j\Delta t$  for  $j \in \mathbb{N}$ . We take  
 455 discrete Fourier transforms

457 
$$u(t) \approx \sum_{j=-M/2}^{M/2-1} \tilde{u}_j e^{ijwt}, \quad \beta(t) \approx \sum_{j=-M/2}^{M/2-1} \tilde{\beta}_j e^{ijwt}, \quad p(t) \approx \sum_{j=-M/2}^{M/2-1} \tilde{p}_j e^{ijwt},$$



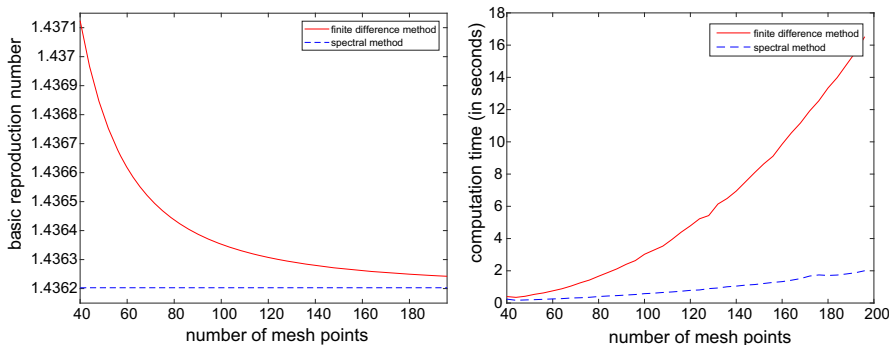


**Fig. 1** Comparison of spectral method and finite difference method (Colour figure online)

458 where the coefficients are given by discrete inverse Fourier transform:

$$459 \quad \tilde{u}_j = \frac{1}{M} \sum_{k=1}^M u(t_k) e^{-ijwt_k}, \quad \tilde{\beta}_j = \frac{1}{M} \sum_{k=1}^M \beta(t_k) e^{-ijwt_k}, \quad \tilde{p}_j = \frac{1}{M} \sum_{k=1}^M p(t_k) e^{-ijwt_k}.$$

460 It is easily seen that  $\tilde{u}_j, \tilde{\beta}_j, \tilde{p}_j$  can be extended as periodic sequence in  $\mathbb{N}$  with the same  
461 period  $M$ . We use the above Fourier transforms to approximate the linear operator  $L$   
462 in (12) as a matrix  $\tilde{L}$  of dimension  $M$ :

$$463 \quad (\tilde{L}\tilde{u})_j = \sum_{\substack{m+n+l=j \\ m,n,l \in [-M/2, M/2-1]}} \theta N \bar{S} \iint_{a,\tau,s \geq 0} e^{-ds + imw(t-s) + ilw(t-s-a-\tau) + inw(t-s-a-\tau)} \\ 464 \quad \tilde{p}_m \tilde{\beta}_l \tilde{u}_n g(a) f(\tau) da d\tau ds \\ 465 \quad = \frac{\theta N \bar{S}}{d + i j w} \sum_{k-n, j-k, n \in [-M/2, M/2-1]} F_k \tilde{\beta}_{k-n} \tilde{p}_{j-k} \tilde{u}_n,$$

467 where  $\tilde{u} = (\tilde{u}_{-M/2}, \dots, \tilde{u}_{M/2-1})^T$  and  $F_k$  is given in (16).

468 To compare the two numerical methods, we consider a toy model:

$$469 \quad \theta = 1, \quad N = 1, \quad \bar{S} = 0.1, \quad T = 2\pi, \quad d = 1, \quad g(a) = e^{-a}, \quad f(\tau) = e^{-\tau},$$

470 and  $\beta(t) = (t - T/2)^2$ ,  $p(t) = t(T - t)$  for  $t \in [0, T]$ . It is observed from numerical  
471 simulation (Fig. 1) that the spectral method is faster and more accurate than the  
472 finite difference method. Notice that this is only a special case with specific data. A  
473 theoretical analysis is required to justify the advantage of spectral method over finite  
474 difference method. We leave this problem for future investigation.

475 **4.4 Examples**

476 In the subsection, we consider three examples: (i) bursting viral production model;  
 477 (ii) budding with constant delay and viral production rate; and (iii) gamma-distributed  
 478 intracellular and viral production.

479 *Example 1 Bursting viral production model*

480 Consider a simple case when the infected cells release all virus particles at a fixed  
 481 age  $\tau_0$ , namely  $\gamma(\tau) = \delta(\tau - \tau_0)$  in the age-structured model, where  $\delta(\tau)$  is the  
 482 Dirac delta mass centered at  $\tau = 0$ . The viral production rate is also a delta function  
 483  $q(a) = N\delta(a)$ . It can be calculated that

$$484 \theta = e^{-\int_0^{\tau_0} \mu_1(a)da}, \quad f(\tau) = \delta(\tau - \tau_0), \quad g(a) = \delta(a).$$

485 The corresponding delay differential system is

$$486 S'(t) = \lambda - \delta S(t) - \beta(t)S(t)V(t), \\ 487 V'(t) = \theta Np(t)\beta(t - \tau_0)S(t - \tau_0)V(t - \tau_0) - dV(t).$$

488 Upon assuming  $p(t), \beta(t)$  are of the small amplitude sinusoidal type (19), we can  
 489 utilize Theorem 5 to obtain the second-order effect on  $R_0$  from the amplitude param-  
 490 eter,  $\varepsilon$ , of the periodic drug efficacies. In particular,  $F_1 = e^{-i\omega\tau_0}$ , which implies  $A =$   
 491  $(1 - |H_1|^2)\cos(\omega\tau_0)$  and  $B = (1 - |H_1|^2)\sin(\omega\tau_0)$ . Note that  $\arctan(B/A) = \omega\tau_0$   
 492 mod  $T$  if  $A \geq 0$ , and  $\arctan(B/A) = \pi + \omega\tau_0$  mod  $T$  if  $A < 0$ . Thus, the optimal  
 493 phase difference between the combination drug treatments with period  $T$  in the case  
 494 of bursting virus model with intracellular delay  $\tau_0$  is  $\phi^* = T/2 + \tau_0 \bmod T$ . The  
 495 intuition for this result can be related to the previous work on the ODE virus model  
 496 (Browne and Pilyugin 2016), which argues that the maximal rates of viral production  
 497 and infection should be de-synchronized to antagonize the virus replication cycle.

498 Here we also bring to attention the recent work by Neagu et al. (2018), exploring  
 499 potential viral evolution of its intracellular delay in order to “resist” antiviral treatment  
 500 for a single drug with periodic efficacy. To find the critical delay from the virus  
 501 perspective in the case of single-drug treatment, consider the special case  $\beta(t) =$   
 502  $1 + 2\varepsilon \cos \omega t$  and  $p(t) = 1$ . Then, it follows that the first term involving  $\varepsilon$  in the  
 503 expansion of  $R_0(\varepsilon)$ , the  $\varepsilon^2$  coefficient  $\rho_{02}$ , can be written as:

$$504 \rho_{02} = \frac{2d [d \cos \omega\tau_0 - \omega \sin \omega\tau_0 - d]}{2d(d - d \cos \omega\tau_0 + \omega \sin \omega\tau_0) + \omega^2} = \left[ -1 + \frac{\omega^2/(2d)}{d \cos \omega\tau_0 - \omega \sin \omega\tau_0 - d} \right]^{-1},$$

505 which achieves its maximum when  $d \cos \omega\tau_0 - \omega \sin \omega\tau_0 = \sqrt{d^2 + \omega^2}$ . Thus, the  
 506 critical delay from the virus perspective can be calculated as  $\tau_0^* = T - \arctan(\omega/d)/\omega$   
 507 mod  $T$ . At this critical value,  $\rho_{02} = 2d/(\sqrt{\omega^2 + d^2} - d)$ . The result concurs with  
 508 simulation and informal arguments in Neagu et al. (2018) showing that the critical  
 509 intracellular delay for the virus is slightly less than drug dosing period, and when

512  $\omega/d$  is small, the offset is close to the (free) virus generation time ( $1/d$ ). Note that an  
 513 objective function different from  $R_0$  was chosen in Neagu et al. (2018) and the offset  
 514 was estimated as  $1/(2d)$ .

515 *Example 2 Budding with constant delay and viral production rate*

516 Assume the infected cells mature at the age  $\tau = \tau_0$  and all mature-infected cells have  
 517 constant death rate and virus production rate; namely, in the age-structured model, we  
 518 have  $\gamma(\tau) = \delta(\tau - \tau_0)$  as before, and  $\mu_2(a) = v$ , and  $q(a) = vN$ . We then have

$$519 \quad \theta = e^{-\int_0^{\tau_0} \mu_1(a) da}, \quad f(\tau) = \delta(\tau - \tau_0), \quad g(a) = v e^{-va}.$$

520 Denote the number of productively infected cells by  $I(t) = \int_0^\infty i(t, a) da$ , we arrive at  
 521 the delay differential system

$$522 \quad S'(t) = \lambda - \delta S(t) - \beta(t)S(t)V(t), \\ 523 \quad I'(t) = \theta\beta(t - \tau_0)S(t - \tau_0)V(t - \tau_0) - vI(t), \\ 524 \quad V'(t) = vNp(t)I(t) - dV(t).$$

525 It is noted that the bursting case in Example 1 is the same as the limiting case of  
 526 budding here in Example 2 with  $v \rightarrow \infty$ . It is easily seen that  $F_1 = ve^{-i\omega\tau_0}/(v + i\omega)$ .  
 527 Recall that  $H_1 = d/(d + i\omega)$ . It is easily seen that

$$529 \quad A = \frac{\omega^2}{d^2 + \omega^2} \cdot \frac{v[\nu \cos(\omega\tau_0) - \omega \sin(\omega\tau_0)]}{v^2 + \omega^2} + \frac{\omega^2}{v^2 + \omega^2} \cdot \frac{d^2}{d^2 + \omega^2}, \\ 530 \quad B = \frac{\omega^2}{d^2 + \omega^2} \cdot \frac{v[\omega \cos(\omega\tau_0) + \nu \sin(\omega\tau_0)]}{v^2 + \omega^2} + \frac{\omega^2}{v^2 + \omega^2} \cdot \frac{-d\omega}{d^2 + \omega^2}.$$

532 Consequently, the optimal phase shift of drug treatments is

$$533 \quad \phi^* = \frac{T}{2} + \frac{T}{2\pi} \arctan \frac{\nu[\omega \cos(\omega\tau_0) + \nu \sin(\omega\tau_0)] - d\omega}{\nu[\nu \cos(\omega\tau_0) - \omega \sin(\omega\tau_0)] + d^2} \mod T$$

535 if  $A \geq 0$ , and

$$536 \quad \phi^* = \frac{T}{2\pi} \arctan \frac{\nu[\omega \cos(\omega\tau_0) + \nu \sin(\omega\tau_0)] - d\omega}{\nu[\nu \cos(\omega\tau_0) - \omega \sin(\omega\tau_0)] + d^2} \mod T$$

538 if  $A < 0$ . Especially, when  $\tau_0 = 0$  (which corresponds to the ODE virus model), the  
 539 above formula reduces to  $\phi^* = \frac{T}{2} + \frac{T}{2\pi} \arctan \frac{\omega(\nu-d)}{\nu^2+d^2} \mod T$ . This concurs with the  
 540 result of global minimization of  $R_0$  at  $\phi^* = T/2$  obtained for bang-bang-type drug  
 541 efficacies in the case of equal infected cell and viral death rates,  $\nu = d$  (Browne and  
 542 Pilyugin 2016).

543 In order to find the critical delay from the virus perspective in the case of single-drug  
 544 treatment, consider the special case  $\beta(t) = 1 + 2\varepsilon \cos \omega t$  and  $p(t) = 1$ . We consider  
 545  $\rho_{02}$  as a function of  $\tau_0$ :

$$\begin{aligned} 546 \quad \rho_{02} &= \frac{2dv \left[ -dv + (dv - \omega^2) \cos \omega \tau_0 - (\omega d + \omega v) \sin \omega \tau_0 \right]}{(dv - \omega^2 - dv \cos \omega \tau_0)^2 + (\omega d + \omega v + dv \sin \omega \tau_0)^2} \\ 547 \quad &= \left[ -1 + \frac{\omega^2(d^2 + \omega^2 + v^2)/(2dv)}{-dv + (dv - \omega^2) \cos \omega \tau_0 - (\omega d + \omega v) \sin \omega \tau_0} \right]^{-1}, \end{aligned}$$

549 which achieves its maximum when

$$550 \quad (dv - \omega^2) \cos \omega \tau_0 - (\omega d + \omega v) \sin \omega \tau_0 = \sqrt{(dv - \omega^2)^2 + (\omega d + \omega v)^2}.$$

551 Thus, the critical delay can be calculated as:

$$552 \quad \tau_0^* = T - \frac{T}{2\pi} \arccos \frac{dv - \omega^2}{\sqrt{(dv - \omega^2)^2 + (\omega d + \omega v)^2}} \mod T.$$

554 We will use the following parameter values representative of HIV infection (Perel-  
 555 son and Nelson 1999) to conduct numerical simulations:

$$\begin{aligned} 556 \quad \lambda &= 10^4, \quad \delta = 0.01, \quad \theta = 0.98, \quad k = 8 \times 10^{-7}, \\ 557 \quad d &= 13, \quad \tau_0 = 2, \quad T = 1, \quad N = 300. \end{aligned} \quad (25)$$

559 For this example, we consider sinusoidal drug efficacies of form (4) with  $\eta_1(t) =$   
 560  $0.945 - 2\varepsilon \cos(\omega t)$  and  $\eta_2(t) = 0$ , where  $\varepsilon = 0.01$  and  $\omega = 2\pi$ . Now, we choose  
 561 different values of  $v$  and vary  $\tau_0$  to see how the time delay affects the basic reproduction  
 562 number, producing the  $T$  – periodic curves  $R_0(\phi)$  displayed in Fig. 2. Again note that  
 563 when  $v \rightarrow \infty$ , the model reduces to the one in Example 1. Observe that the amplitude  
 564 of  $R_0(\tau_0)$  increases and the critical delay  $\tau_0^*$  shifts closer to being synchronized with  
 565 the period  $T$  as  $v \rightarrow \infty$ .

566 Next we consider periodic combination drug therapy, setting  $\eta_i(t) = 0.765 -$   
 567  $2\varepsilon \cos(\omega t)$  with  $\varepsilon = 0.05$ , and consider the effect of varying phase difference  $\phi$   
 568 between drug efficacies,  $\eta_1(t)$  and  $\eta_2(t - \phi)$ , on  $R_0$ . In Fig. 3a, we plot  $R_0$  as a  
 569 function of the phase shift  $\phi$  with different values of  $v$  for the case  $\tau_0 = 1.9283$ .  
 570 Note that this is the critical viral delay,  $\tau_0^*$ , when  $v \rightarrow \infty$  in the case of single-drug  
 571 therapy shown in Fig. 2. Notice that in the viral bursting case ( $v \rightarrow \infty$ ), the phase  
 572 difference  $\phi$  substantially affects  $R_0$ . In particular, if the P-inhibitor is introduced at  
 573  $\phi = 0.5$ ,  $R_0$  reduces to below one, as opposed to either the single-drug (maximal  $R_0$ )  
 574 or in-phase ( $\phi = 0$ ) scenario. Thus, if the virus optimizes its  $R_0$  under single-drug  
 575 therapy as discussed in Neagu et al. (2018), it is still possible to effectively antagonize  
 576 the virus with a correctly timed distinct antiviral drug. Also, observe in this case, as  
 577 we decrease  $v$ , the amplitude of  $R_0(\phi)$  decreases. In Fig. 3b, we consider the case  
 578  $\tau_0 = 1.6$ . The curves of  $R_0(\phi)$  change substantially from the prior case, showing  
 579 the sensitivity of  $R_0$  to both  $\tau_0$  and  $\phi$ . We observe from Fig. 3 that as  $v$  increases,

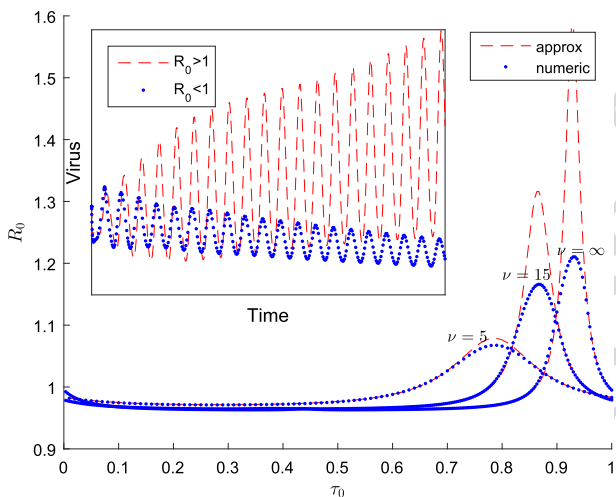


**Fig. 2** The basic reproduction number  $R_0$  as a function of the maturation delay  $\tau_0$ . The numeric values are computed using both finite difference and spectral methods with sufficiently many mesh points such that the graphs obtained from both methods are almost the same. In the subfigure, we set  $\nu = 15$  and choose  $\tau_0 = 0.7$  (blue dotted curve) and  $\tau_0 = 0.8$  (red dashed curve), respectively, to calculate the viral population along the time

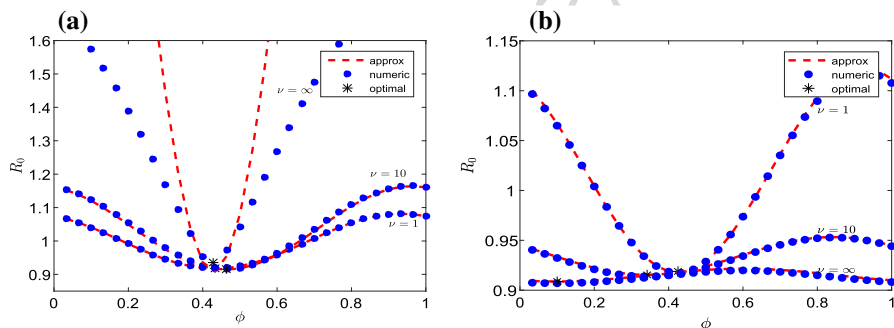


**Fig. 3** The basic reproduction number  $R_0$  as a function of the phase shift  $\phi$  for **a**  $\tau_0 = 1.9283$  and **b**  $\tau_0 = 1.6$ . The numeric values are computed using both finite difference and spectral methods with sufficiently many mesh points such that the graphs obtained from both methods are almost the same (Colour figure online)

580 both average and amplitude of  $R_0$  decrease, and the optimal  $\phi^*$  shifts to the left, even  
 581 though the reproduction number corresponding to the case with constant drug efficacy  
 582 ( $\varepsilon = 0$ ) remains fixed.

583 *Example 3 Gamma-distributed intracellular and viral production*

584 Recent studies have shown for HIV the intracellular and viral production kernels may  
 585 be gamma-distributed (Beauchemin et al. 2017). Thus, we let

$$586 \quad f(\tau) = \frac{\tau^{k_1-1} e^{-\tau/\theta_1}}{\Gamma(k_1)\theta_1^{k_1}}, \quad g(a) = \frac{a^{k_2-1} e^{-a/\theta_2}}{\Gamma(k_2)\theta_2^{k_2}}.$$

587 For illustration, we consider the simple case when  $k_1 = k_2 = 1$ . Define

588 
$$I(t) = \theta \theta_2 \int_0^\infty \int_0^\infty g(a) f(\tau) \beta(t-a-\tau) S(t-a-\tau) V(t-a-\tau) d\tau da$$

589 and  $E(t) = \theta_1 \int_0^\infty f(\tau) \beta(t-\tau) S(t-\tau) V(t-\tau) d\tau$ . We transform the delay differential  
590 system into an ordinary differential system:

591 
$$\begin{aligned} S'(t) &= \lambda - \delta S(t) - \beta(t) S(t) V(t), \\ 592 E'(t) &= \beta(t) S(t) V(t) - E(t)/\theta_1, \\ 593 I'(t) &= \theta E(t)/\theta_1 - I(t)/\theta_2, \\ 594 V'(t) &= p(t) N I(t)/\theta_2 - d V(t). \end{aligned} \quad (26)$$

595 This is equivalent to the age-structured PDE (3) with

596 
$$\gamma(\tau) = \theta/\theta_1, \quad \mu_1(\tau) = (1-\theta)/\theta_1, \quad q(a) = N/\theta_2, \quad \mu_2(a) = 1/\theta_2.$$

597 Similarly, for any positive integers  $k_1$  and  $k_2$ , we can use linear chain trick (Smith  
598 2011) to obtain a system of  $k_1 + k_2 + 2$  ordinary differential equations. However, we  
599 assume  $k_1$  and  $k_2$  are positive real numbers, and thus, the model system is in general  
600 still of infinite dimension. It can be calculated that

601 
$$F_1 = (1 + i\theta_1\omega)^{-k_1} (1 + i\theta_2\omega)^{-k_2} = |F_1| e^{-i(\omega_1 k_1 + \omega_2 k_2)},$$

602 where  $|F_1| = [1 + (\theta_1\omega)^2]^{-k_1/2} [1 + (\theta_2\omega)^2]^{-k_2/2}$ ,  $\omega_1 = \arctan(\theta_1\omega)$  and  $\omega_2 =$   
603  $\arctan(\theta_2\omega)$ . A further computation gives

604 
$$\begin{aligned} 605 A &= \frac{\omega^2}{d^2 + \omega^2} \cdot |F_1| \cos(\omega_1 k_1 + \omega_2 k_2) + (1 - |F_1|^2) \cdot \frac{d^2}{d^2 + \omega^2}, \\ 606 B &= \frac{\omega^2}{d^2 + \omega^2} \cdot |F_1| \sin(\omega_1 k_1 + \omega_2 k_2) + (1 - |F_1|^2) \cdot \frac{-d\omega}{d^2 + \omega^2}. \end{aligned}$$

607 Consequently, the optimal phase shift of drug treatments is

608 
$$\phi^* = \frac{T}{2} + \frac{T}{2\pi} \arctan \frac{\omega^2 |F_1| \sin(\omega_1 k_1 + \omega_2 k_2) - d\omega (1 - |F_1|^2)}{\omega^2 |F_1| \cos(\omega_1 k_1 + \omega_2 k_2) + d^2 (1 - |F_1|^2)} \mod T$$

609 if  $A \geq 0$ , and

610 
$$\phi^* = \frac{T}{2\pi} \arctan \frac{\omega^2 |F_1| \sin(\omega_1 k_1 + \omega_2 k_2) - d\omega (1 - |F_1|^2)}{\omega^2 |F_1| \cos(\omega_1 k_1 + \omega_2 k_2) + d^2 (1 - |F_1|^2)} \mod T$$

611 if  $A < 0$ .

612 For numerical simulations in this example, we consider more realistic drug efficacies given by the impulsive exponential decay dose-response form (5) as in Vaidya and

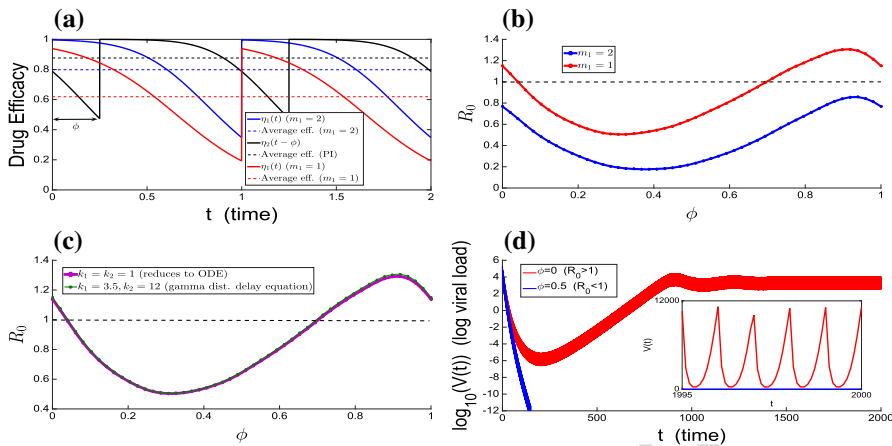


**Fig. 4** **a** Impulsive exponential decay dose-response drug efficacies of RTI (blue or red) and PI (black). The pharmacodynamic parameters used in simulations from formula (5) are  $m_1 = 1$  (red) or 2 (blue),  $m_2 = 3$ , and  $r_i = 6 \ln 2$ ,  $C_{\max_i} / IC_{50_i} = 15$  for  $i = 1, 2$ . **b**  $R_0$  as a function of phase difference  $\phi$  for the cases  $m_1 = 1$  (red) or 2 (blue). The gamma distribution parameters are  $k_1 = 3.5$ ,  $k_2 = 12$  and HIV parameters are given in text. **c**  $R_0$  as a function of phase difference  $\phi$  when  $m_1 = 1$  for gamma distribution parameters  $k_1 = k_2 = 1$  and  $k_1 = 3.5$ ,  $k_2 = 12$ . **d** Simulations of time-dependent solutions displaying virus level when  $k_1 = k_2 = 1$  for in-phase ( $\phi = 0$ ) and out-of-phase ( $\phi = 0.5$ ) drug combination

618 Rong (2017). The pharmacodynamic parameters chosen are consistent with antiviral  
 619 medications (RTIs and PIs) for HIV studied in Shen et al. (2008). For the RTI drug  
 620 class, we consider two different types, NRTIs and NNRTIs, which have different slope  
 621 parameters,  $m_1$ , in (5). In particular, we take  $m_1 = 1$  or 2 in simulations, with the larger  
 622  $m_1$  value increasing the drug efficacy. Figure 4a displays the periodic drug efficacies  
 623 utilized for the RTI,  $\eta_1(t)$  (for the 2 different  $m_1$  values), and the PI,  $\eta_2(t - \phi)$ . The  
 624 baseline HIV parameter values are kept as (25). Furthermore, we choose the gamma  
 625 distribution parameters in line with the recent experimental estimates obtained for SIV  
 626 parameters (Beauchemin et al. 2017). In particular,

$$627 \quad k_1 = 3.5, \quad k_2 = 12, \quad \theta_1 = \tau_0/k_1 = 0.57, \quad \theta_2 = 1/(k_2 v) = 0.12.$$

628 In Fig. 4b, we plot the basic reproduction number as a function of the phase difference  
 629  $\phi$  for  $m_1 = 1$  and 2. Next for the case where  $m_1 = 2$ , in Fig. 4c, we also plot  $R_0$  for  
 630 gamma distribution parameters  $k_1 = 1$ ,  $k_2 = 1$ ,  $\theta_1 = \tau_0/k_1 = 2$ ,  $\theta_2 = 1/(k_2 v) = 1$ ,  
 631 corresponding to the analogous ODE (26). Observe that the optimal phase shifts are  
 632 almost the same and the optimal values of basic reproduction number are nearly  
 633 identical. Thus, in terms of  $R_0$ , the ODE can be a good approximation of the infinite-  
 634 dimensional equations corresponding to fitted parameters. The ODE case also has  
 635 the advantage of relative ease in conducting numerical simulations. Thus, we display  
 636 time-dependent solutions in Fig. 4d illustrating how the phase difference critically  
 637 affects the outcomes of viral persistence versus extinction corresponding to whether  
 638  $R_0$  is greater or less than unity.

## 639 5 Discussion

640 In this paper, we studied within-host viral dynamics under general intracellular dis-  
641 tributed delays and periodic combination antiretroviral therapy. Our formulation  
642 extends previous models by inclusion of eclipse and viral production stages as probabili-  
643 ty distributions, along with time-varying drug treatments. This allows us to incorporate  
644 recent experimentally derived gamma distribution parameters of HIV replication  
645 (Beauchemin et al. 2017) and pharmacodynamic models of drug therapy. Further-  
646 more, to the best of our knowledge, we provide the first rigorous analysis establishing  
647 the basic reproduction number  $R_0$  as a global threshold determining extinction versus  
648 persistence in an infinite-dimensional virus model with intracellular delay and periodic  
649 antiviral treatment. Although an explicit formula is not possible, we utilize Fourier  
650 analysis to provide an effective method of analytical and numerical approximation of  
651  $R_0$ . In the proof of persistence theorem, we chose to construct an autonomous semiflow  
652 as in Saperstone (1981). It is worth mentioning that one may use another approach by  
653 considering the associated Poincaré (time-periodic) map (Zhao 2017b).

654 Motivated by previous results demonstrating large impacts on periodic viral dynam-  
655 ics induced by varying intracellular delays (Neagu et al. 2018) or phase shifts in  
656 combination drug therapy (Browne and Pilyugin 2012), we characterize how the tim-  
657 ing of, both, viral replication cycle and combination antiviral regimen can critically  
658 affect  $R_0$ . Our analytical and numerical results show that a combination therapy can  
659 effectively neutralize a virus by optimizing phase difference  $\phi$  between two distinct  
660 antivirals, even in the case that the virus adapts to a single drug through “synchroniz-  
661 ing” its intracellular delay  $\tau_0$  with dosing period, as in Neagu et al. (2018). The phase  
662 difference  $\phi$  between antiviral drug efficacies substantially affects  $R_0$  in simulations  
663 with realistic pharmacokinetics and gamma-distributed viral production delays for  
664 HIV (Fig. 4). Thus, consideration of pharmacodynamics and dosing regimen together  
665 with viral replication kinetics may be important for the optimization of treatment.

666 There are several limitations to our model (9), which can be further addressed. First,  
667 as already mentioned in Remark 1, more detailed models of the viral replication cycle  
668 can allow for the precise mode of action of specific antiviral medications (e.g., RTIs). In  
669 “Appendix A”, we show that assuming a fixed (discrete) intracellular delay for reverse  
670 transcription (RT) simply shifts the action of an RTI by this delay duration in our  
671 analyzed model (9); however, more general RT delay distributions will require analysis  
672 of the extended model. Additionally, although our model predicts the clearance of the  
673 virus when  $R_0 < 1$ , current treatment for HIV cannot eradicate the virus due to latently  
674 infected cells which are not targeted by antiviral therapy. Recent studies have modeled  
675 HIV persistence and the latent reservoir (Rong and Perelson 2009), which provides  
676 motivation for extending our model to include latency. Finally, drug resistance may be a  
677 barrier to treatment success and will be studied in future research into the optimization  
678 of antiviral therapies.

679 **Acknowledgements** We would like to express our gratitude to the anonymous referees for careful reading  
680 and helpful suggestions which help to improve the presentation of this paper. HS was partially supported by  
681 the National Natural Science Foundation of China (Nos. 11971285, 11601392), Shaanxi Hundred-Talent  
682 Program, and the Fundamental Research Funds for the Central Universities (No. GK201902005). XP was

683 partially supported by a grant from China Scholarship Council. CJB was partially supported by a US  
 684 National Science Foundation grant (DMS-1815095).

## 685 A Extended Model with Reverse Transcription

686 We consider the following generalization of (3) with extra compartment explicitly  
 687 tracking the process of reverse transcription (RT) during the eclipse phase of infected  
 688 cell. Thus, the infected cells in the eclipse phase,  $j(t, \tau)$ , are separated into two classes  
 689  $j_1(t, \tau_1)$  and  $j_2(t, \tau_2)$  measuring infected cells  $\tau_1$  units of time after cell infection,  
 690 before RT, and  $\tau_2$  units of time after RT, respectively. Then, the eclipse phase-infected  
 691 cell equation in (3) is modified as follows:

$$692 \quad \left( \frac{\partial}{\partial t} + \frac{\partial}{\partial \tau_1} \right) j_1(t, \tau_1) = -(v_1(\tau_1) + \gamma_1(\tau_1)) j_1(t, \tau_1), \quad j_1(t, 0) = k S(t) V(t), \\ 693 \quad \left( \frac{\partial}{\partial t} + \frac{\partial}{\partial \tau} \right) j_2(t, \tau) = -(v_2(\tau) + \gamma_2(\tau)) j_2(t, \tau), \\ 694 \quad j_2(t, 0) = (1 - \eta_1(t)) \int_0^\infty \gamma_1(\tau_1) j_1(t, \tau_1) d\tau_1, \\ 695 \quad \left( \frac{\partial}{\partial t} + \frac{\partial}{\partial a} \right) i(t, a) = -\mu(a) i(t, a), \quad i(t, 0) = \int_0^\infty \gamma_2(\tau) j_2(t, \tau) d\tau. \\ 696$$

697 In the special case that  $\gamma_1(\tau_1) = \delta(\tau_1 - r)$ , then we have

$$698 \quad j_2(t, 0) = (1 - \eta_1(t)) e^{-\int_0^r v_1(s) ds} k S(t - r) V(t - r),$$

699 which implies that

$$700 \quad j_2(t, \tau_2) = k(1 - \eta_1(t - \tau_2)) e^{-\int_0^r v_1(s) ds} S(t - \tau_2 - r) V(t - \tau_2 - r) \\ 701 \quad e^{-\int_0^{\tau_2} (v_2(s) + \gamma_2(s)) ds} \\ 702 \quad = k(1 - \eta_1(t - \tau + r)) e^{-\int_0^r v_1(s) ds} S(t - \tau) V(t - \tau) e^{-\int_0^{\tau-r} (v_2(s) + \gamma_2(s)) ds},$$

704 where  $\tau := \tau_2 + r$ . Consequently, the differential equation for  $V(t)$  becomes

$$705 \quad V'(t) = p(t) \int_0^\infty \int_0^\infty q(a) e^{-\int_0^a \mu(s) ds} \gamma_2(\tau) e^{-\int_0^r v_1(s) ds - \int_0^{\tau-r} (v_2(s) + \gamma_2(s)) ds} \beta(t - a - \tau + r) \\ 708 \quad S(t - a - \tau) V(t - a - \tau) d\tau da - dV,$$

708 which is the same as Eq. (9) with the effective infection rate (affected by the RT  
 709 inhibitor) shifted by  $r$  units of time, i.e.,  $\tilde{\beta}(t) = \beta(t + r)$ . The corresponding

710 relation between PDE and DDE is:  $P(\tau) = e^{-\int_0^r v_1(s)ds - \int_0^{\tau-r} v_2(s)ds}$  and  $\pi(\tau) =$   
 711  $\gamma_2(\tau)e^{-\int_0^{\tau-r} \gamma_2(s)ds}$ ,  $\theta := \int_0^{\infty} P(\tau)\pi(\tau)d\tau$ ,  $f(\tau) = (P(\tau)\pi(\tau))/\theta$ , along with  $g(a) =$   
 712  $(q(a)\sigma(a))/N$ ,  $N = \int_0^{\infty} q(a)\sigma(a)da$  where  $\sigma(a) = e^{-\int_0^a \mu(s)ds}$ .

## B Proof of Theorem 4

714 We proceed in the following steps.

715 1. In Sect. 3.1, we have proved that  $\Psi(t)$  is point dissipative and the trajectories of  
 716 any given bounded set are uniformly bounded.  
 717 2. We show that  $\Psi(t)$  is asymptotically smooth.

718 Fix  $C > \lambda/\min\{\delta, d\}$ . It follows from Burton and Hutson (1989), Lemma 3.2 that  
 719 the set

$$720 B_C := \{u \in C_{\alpha}^+ : \sup_{\theta \leq 0} u(\theta)e^{\alpha\theta/2} \leq C\}$$

721 is compact in  $C_{\alpha}^+$ . We need to prove that  $B_C \times B_C \times \mathbb{R}_T$  attracts all bounded invariant  
 722 set  $\Gamma$  in  $X = C_{\alpha}^+ \times C_{\alpha}^+ \times \mathbb{R}_T$ . Fix any  $(S_r, V_r, r)$  in  $\Gamma$ , we denote  $(S_t, V_t, t+r) =$   
 723  $\Psi(t)(S_r, V_r, r)$  such that  $(S(t), V(t)) = (S_t(0), V_t(0))$  satisfies system (8), (9) for  
 724  $t > r$  with the initial condition  $(S(r+\theta), V(r+\theta)) = (S_r(\theta), V_r(\theta))$  for  $\theta \leq 0$ .  
 725 Since the limit superior of  $S(t)$  is bounded above by  $\lambda/\delta$ , we have  $S(t) < C$  for all  
 726 large  $t$ . Let  $t_0 \geq 0$  be the largest  $t \geq r$  such that  $S(t) \geq C$ . If  $S(t) < C$  for all  
 727  $t \geq r$ , we set  $t_0 = r$ . For  $t > t_0$ , define

$$728 u_t(\theta) := \begin{cases} S_t(\theta), & t_0 - t \leq \theta \leq 0, \\ S(t_0)e^{-\alpha(\theta-t_0+t)/2}, & \theta \leq t_0 - t. \end{cases}$$

730 It is readily seen that  $u_t \in B_C$ . Now, we intend to show that  $\|u_t - S_t\|_{\alpha} \rightarrow 0$  as  
 731  $t \rightarrow \infty$ . For  $\theta \in [t_0 - t, 0]$ , we have  $u_t(\theta) = S_t(\theta)$ . As  $t \rightarrow \infty$ , we have

$$732 u_t(\theta)e^{\alpha\theta} = S(t_0)e^{\alpha(\theta+t_0-t)/2} \leq Ce^{\alpha(t_0-t)} \rightarrow 0, \theta \leq t_0 - t; \\ 733 S_t(\theta)e^{\alpha\theta} \leq S(t+\theta)e^{\alpha(t_0-t)} \leq \sup_{r \leq s \leq t_0} S(s)e^{\alpha(t_0-t)} \rightarrow 0, \theta \in [r-t, t_0-t]; \\ 734 S_t(\theta)e^{\alpha\theta} = S_r(t-r+\theta)e^{\alpha(\theta+t-r)}e^{-\alpha(t-r)} \leq \|S_r\|_{\alpha}e^{-\alpha(t-r)} \rightarrow 0, \theta \leq r-t.$$

736

Therefore,

737

$$\|u_t - S_t\|_\alpha = \sup_{\theta \leq t_0 - t} |u_t(\theta) - S_t(\theta)| e^{\alpha\theta} \\ \leq C e^{\alpha(t_0 - t)} + \max\{\sup_{r \leq s \leq t_0} S(s) e^{\alpha(t_0 - t)}, \|S_r\|_\alpha e^{-\alpha(t-r)}\} \rightarrow 0,$$

738

739

740 as  $t \rightarrow \infty$ . Similarly, we define

741

742

$$v_t(\theta) := \begin{cases} V_t(\theta), & t_1 - t \leq \theta \leq 0, \\ V(t_1) e^{-\alpha(\theta - t_1 + t)/2}, & \theta \leq t_1 - t, \end{cases}$$

743

744

745

746

where  $t_1$  is the largest  $t \geq r$  such that  $V(t) \geq C$ ; if  $V(t) < C$  for all  $t \geq r$ , then we set  $t_1 = r$ . It can be shown that  $v_t \in B_C$  and  $\|v_t - V_t\|_\alpha \rightarrow 0$  as  $t \rightarrow \infty$ . Therefore, the compact set  $B_C \times B_C \times \mathbb{R}_T$  attracts all bounded invariant set  $\Gamma \in X$ , which proves asymptotic smoothness of system (8), (9).

747

748

749

750

751

752

753

3. By Hale and Waltman (1989), Theorem 2.1,  $\Psi(t)$  possesses a nonempty global attractor in  $X$ . Denote  $X_0 = \{(u, v, r) \in X : v(0) > 0\}$  and  $\partial X_0 = X \setminus X_0 = \{(u, v, r) \in X : v(0) = 0\}$ . Introduce a generalized distance function  $p : X \rightarrow \mathbb{R}_+$  as  $p(u, v, r) = v(0)$ . It is readily seen that  $p^{-1}(0) = \partial X_0$  and  $p^{-1}(0, \infty) = X_0$ . Furthermore, by comparison principle,  $p(\Psi(t)x) > 0$  for all  $x \in X_0$ . Hence, the condition (P) in Smith and Zhao (2001), Section 3 is verified; see also Zhao (2017b), Definition 1.3.1.

754

755

756

757

758

759

We now prove that the basin of attraction for  $E_0 \times \mathbb{R}_T$  does not intersect  $p^{-1}(0, \infty) = X_0$ . Assume to the contrary that there exists  $(S_0, V_0, t_0) \in X_0$  such that  $(S(t), V(t)) \rightarrow (\bar{S}, 0)$  as  $t \rightarrow \infty$ , where  $(S(t), V(t)) = (S_t(0), V_t(0))$  with  $(S_t, V_t) = U(t, t_0)(S_0, V_0)$ . Since  $V(0) > 0$ , comparison principle shows that  $V(t) > 0$  for all  $t \geq 0$ . For any  $\mu, \nu > 0$ , we introduce a parametrized operator on  $\mathbb{P}_T$ :

760

$$(L_{\mu, \nu}\phi)(t) = \theta N \bar{S} \int_0^\infty \int_0^\infty \int_0^\infty e^{-\mu(s+a+\tau)-(d+\nu)s} p(t-s) g(a) f(\tau) \beta(t-s-a-\tau) \\ \phi(t-s-a-\tau) d\tau da ds.$$

761

762

763

764

765

766

Clearly,  $\rho(L_{0,0}) = R_0 > 1$ . It follows from continuity (Degla 2008, Theorem 2.1) and monotonicity (Burlando 1991, Theorem 1.1) of  $L_{\mu, \nu}$  on both  $\mu$  and  $\nu$  that  $\rho(L_{\delta, \delta}) > 1$  for some small  $\delta > 0$ . Krein–Rutman theorem guarantees that the principal eigenfunction  $\phi$  of  $L_{\delta, \delta}$  is positive. Set  $\varepsilon = \bar{S} - \bar{S}/\rho(L_{\delta, \delta}) > 0$  and  $v(t) = e^{\delta t} \phi(t)$ . It is easily seen that

767

$$v(t) = \theta N (\bar{S} - \varepsilon) \int_0^\infty \int_0^\infty \int_0^\infty e^{-(d+\delta)s} p(t-s) g(a) f(\tau) \beta(t-s-a-\tau) \\ v(t-s-a-\tau) d\tau da ds.$$

768

769 Differentiating both sides gives a periodic renewal equation

$$770 \quad v'(t) = -(d + \delta)v(t) + \theta N(\bar{S} - \varepsilon)p(t) \int_0^\infty \int_0^\infty \beta(t - a - \tau)g(a)f(\tau) \\ 771 \quad v(t - a - \tau)dad\tau.$$

773 Since  $S(t) \rightarrow \bar{S}$  as  $t \rightarrow \infty$ , there exists  $t_0 > 0$  such that  $S(t) > \bar{S} - \varepsilon$  for all  
774  $t > t_0$ . Define

$$775 \quad F(t) = \theta N(\bar{S} - \varepsilon)p(t) \iint_{\tau+a \geq t-t_0} \beta(t - a - \tau)g(a)f(\tau)v(t - a - \tau)dad\tau.$$

776 It is easy to show that  $F(t) \rightarrow 0$  as  $t \rightarrow \infty$ . On the other hand,  $v(t) = e^{\delta t}\phi(t) \rightarrow$   
777  $\infty$  as  $t \rightarrow \infty$ . There exists  $t_1 > t_0$ , such that  $F(t) < \delta v(t)$  for all  $t > t_1$ .  
778 Consequently, we obtain

$$779 \quad v'(t) \leq -dv(t) + \theta N(\bar{S} - \varepsilon)p(t) \iint_{\tau+a \leq t-t_0} \beta(t - a - \tau)g(a)f(\tau) \\ 780 \quad v(t - a - \tau)dad\tau$$

781 for all  $t \geq t_1$ . On the other hand,

$$782 \quad V'(t) \geq -dV(t) + \theta N(\bar{S} - \varepsilon)p(t) \iint_{\tau+a \leq t-t_0} \beta(t - a - \tau)g(a)f(\tau) \\ 783 \quad V(t - a - \tau)dad\tau$$

784 for all  $t \geq t_1$ . Let  $C = \max_{t \in [t_0, t_1]} [v(t)/V(t)]$ . It follows from comparison principle  
785 that  $CV(t) \geq v(t)$  for all  $t \geq t_0$ . This leads to a contradiction because  $v(t)$   
786 is unbounded but  $V(t)$  vanishes as  $t \rightarrow \infty$ .

787 4. We demonstrate that  $E_0 \times \mathbb{R}_T$  is isolated and acyclic.

788 Obviously,  $E_0 \times \mathbb{R}_T$  is isolated. If to the contrary  $E_0 \times \mathbb{R}_T$  is cyclic, namely, there  
789 exists a homoclinic orbit  $\{S(t), V(t)\}$  that connects  $E_0$  as  $t \rightarrow \pm\infty$ . We claim that  
790  $V(t) = 0$  for all  $t$ . Otherwise, if  $V(t_0) > 0$  for some  $t_0 \in \mathbb{R}$ , then by (9),  $V(t) > 0$   
791 for all  $t \geq t_0$ . A similar argument as in the previous step shows that  $V(t)$  cannot  
792 converge to 0 at infinity. Hence,  $V(t) = 0$  for all  $t$ , which reduces (8) to a single  
793 ordinary equation and contradicts to the existence of homoclinic orbit.

794 5. All the conditions in Smith and Zhao (2001), Theorem 4.7 (see also Zhao 2017b,  
795 Theorem 1.3.2) have been verified. Therefore, there exists  $\delta_0 > 0$  such that  
796  $\liminf_{t \rightarrow \infty} p(\Psi(t)x) > \delta_0$  for any  $x \in X_0$ . Let  $(S, V)$  be the solution of (8),  
797 (9) with the initial condition  $(u_0, v_0) \in C_\alpha \times C_\alpha$  such that  $v_0(0) > 0$ . Denote  
798  $S_t(\theta) = S(t + \theta)$  and  $V_t(\theta) = V(t + \theta)$  for all  $t \geq 0$  and  $\theta \leq 0$ . We then have  
799  $(u_0, v_0, 0) \in X_0$  and  $(S_t, V_t, t) = \Psi(t)(u_0, v_0, 0)$ . The persistent of  $\Psi(t)$  with  
800 respect to the distance function  $p$  implies that  $\liminf_{t \rightarrow \infty} V(t) > \delta_0$ . By choosing  
801  $\delta_0 > 0$  sufficiently small (and still independent of initial condition), we also obtain  
802 from (8) that  $\liminf_{t \rightarrow \infty} S(t) > \delta_0$ . This completes the proof.

803 **References**

804 Adams B, Banks H, Davidian M, Kwon H-D, Tran H, Wynne S, Rosenberg E (2005) HIV dynamics:  
 805 modeling, data analysis, and optimal treatment protocols. *J Comput Appl Math* 184(1):10–49

806 Bacaër N (2007) Approximation of the basic reproduction number  $R_0$  for vector-borne diseases with a  
 807 periodic vector population. *Bull Math Biol* 69(3):1067–1091

808 Bacaër N, Abdurahman X (2008) Resonance of the epidemic threshold in a periodic environment. *J Math  
 809 Biol* 57(5):649

810 Bacaër N, Dads EHA (2012) On the biological interpretation of a definition for the parameter  $R_0$  in periodic  
 811 population models. *J Math Biol* 65(4):601–621

812 Bacaër N, Oufkri R (2007) Growth rate and basic reproduction number for population models with a simple  
 813 periodic factor. *Math Biosci* 210(2):647–658

814 Beauchemin CA, Miura T, Iwami S (2017) Duration of SHIV production by infected cells is not expo-  
 815 nentially distributed: implications for estimates of infection parameters and antiviral efficacy. *Sci Rep*  
 816 7:42765

817 Browne CJ, Pilyugin SS (2012) Periodic multidrug therapy in a within-host virus model. *Bull Math Biol*  
 818 74(3):562–589

819 Browne CJ, Pilyugin SS (2013) Global analysis of age-structured within-host virus model. *Discrete Contin  
 820 Dyn Syst Ser B* 18(8):1999–2017

821 Browne CJ, Pilyugin SS (2016) Minimizing  $R_0$  for in-host virus model with periodic combination antiviral  
 822 therapy. *Discrete Contin Dyn Syst Ser B* 21(10):3315–3330

823 Buonomo B, Vargas-De-León C (2012) Global stability for an HIV-1 infection model including an eclipse  
 824 stage of infected cells. *J Math Anal Appl* 385(2):709–720

825 Burlando L (1991) Monotonicity of spectral radius for positive operators on ordered Banach spaces. *Arch  
 826 Math* 56:49–57

827 Burton T, Hutson V (1989) Repellers in systems with infinite delay. *J Math Anal Appl* 137(1):240–263

828 Culshaw RV, Ruan S (2000) A delay-differential equation model of HIV infection of CD4<sup>+</sup> T-cells. *Math  
 829 Biosci* 165(1):27–39

830 De Leenheer P (2009) Within-host virus models with periodic antiviral therapy. *Bull Math Biol* 71(1):189–  
 831 210

832 Degla G (2008) An overview of semi-continuity results on the spectral radius and positivity. *J Math Anal  
 833 Appl* 338:101–110

834 Du Y (2006) Order structure and topological methods in nonlinear partial differential equations, vol. 1: max-  
 835 imum principles and applications, volume 2 of series in partial differential equations and applications.  
 836 World Scientific Publishing Co. Pte Ltd., Hackensack

837 Hale JK, Waltman P (1989) Persistence in infinite-dimensional systems. *SIAM J Math Anal* 20(2):388–395

838 Huang G, Liu X, Takeuchi Y (2012) Lyapunov functions and global stability for age-structured HIV infection  
 839 model. *SIAM J Appl Math* 72(1):25–38

840 Neagu IA, Olejjarz J, Freeman M, Rosenbloom DI, Nowak MA, Hill AL (2018) Life cycle synchronization  
 841 is a viral drug resistance mechanism. *PLoS Comput Biol* 14(2):e1005947

842 Nelson PW, Gilchrist MA, Coombs D, Hyman JM, Perelson AS (2004) An age-structured model of HIV  
 843 infection that allows for variations in the production rate of viral particles and the death rate of  
 844 productively infected cells. *Math Biosci Eng* 1(2):267–288

845 Nelson PW, Perelson AS (2002) Mathematical analysis of delay differential equation models of HIV-1  
 846 infection. *Math Biosci* 179(1):73–94

847 Perelson AS, Nelson PW (1999) Mathematical analysis of HIV-1 dynamics in vivo. *SIAM Rev* 41(1):3–44

848 Perelson AS, Neumann AU, Markowitz M, Leonard JM, Ho DD (1996) HIV-1 dynamics in vivo: virion  
 849 clearance rate, infected cell life-span, and viral generation time. *Science* 271(5255):1582–1586

850 Posny D, Wang J (2014) Computing the basic reproductive numbers for epidemiological models in nonho-  
 851 mogeneous environments. *Appl Math Comput* 242:473–490

852 Rebelo C, Margheri A, Bacaër N (2014) Persistence in some periodic epidemic models with infection age  
 853 or constant periods of infection. *Discrete Contin Dyn Syst Ser B* 19:1155–1170

854 Rong L, Feng Z, Perelson AS (2007) Mathematical analysis of age-structured HIV-1 dynamics with com-  
 855 bination antiretroviral therapy. *SIAM J Appl Math* 67(3):731–756

856 Rong L, Perelson AS (2009) Modeling HIV persistence, the latent reservoir, and viral blips. *J Theor Biol*  
 857 260(2):308–331

858 Saperstone SH (1981) Semidynamical systems in infinite-dimensional spaces, vol 37. Applied mathematical  
859 sciences. Springer, New York

860 Shen L, Peterson S, Sedaghat AR, McMahon MA, Callender M, Zhang H, Zhou Y, Pitt E, Anderson KS,  
861 Acosta EP et al (2008) Dose-response curve slope sets class-specific limits on inhibitory potential of  
862 anti-HIV drugs. *Nat Med* 14(7):762

863 Shu H, Wang L, Watmough J (2013) Global stability of a nonlinear viral infection model with infinitely  
864 distributed intracellular delays and CTL immune responses. *SIAM J Appl Math* 73(3):1280–1302

865 Smith HL (2011) An introduction to delay differential equations with applications to the life sciences, vol  
866 57. Springer, New York

867 Smith HL, Zhao X-Q (2001) Global attractors and steady states for uniformly persistent dynamical systems.  
868 *Nonlinear Anal* 47:6169–6179

869 Vaidya NK, Rong L (2017) Modeling pharmacodynamics on HIV latent infection: choice of drugs is key  
870 to successful cure via early therapy. *SIAM J Appl Math* 77(5):1781–1804

871 Wang J, Dong X (2018) Analysis of an HIV infection model incorporating latency age and infection age.  
872 *Math Biosci Eng* 15(3):569–594

873 Wang X, Liu S, Rong L (2014) Permanence and extinction of a non-autonomous HIV-1 model with time  
874 delays. *Discrete Contin Dyn Syst Ser B* 19(6):1783

875 Wang X, Song X, Tang S, Rong L (2016) Dynamics of an HIV model with multiple infection stages and  
876 treatment with different drug classes. *Bull Math Biol* 78(2):322–349

877 Wang Z, Zhao X-Q (2013) A within-host virus model with periodic multidrug therapy. *Bull Math Biol*  
878 75(3):543–563

879 Wei X, Ghosh SK, Taylor ME, Johnson VA, Emini EA, Deutsch P, Lifson JD, Bonhoeffer S, Nowak MA,  
880 Hahn BH et al (1995) Viral dynamics in human immunodeficiency virus type 1 infection. *Nature*  
881 373(6510):117

882 Xu D, Zhao X-Q (2005) Dynamics in a periodic competitive model with stage structure. *J Math Anal Appl*  
883 311(2):417–438

884 Zhao X-Q (2017) Basic reproduction ratios for periodic compartmental models with time delay. *J Dyn  
885 Differ Equ* 29(1):67–82

886 Zhao X-Q (2017) Dynamical systems in population biology. In: Sinclair N, Pimm D, Higginson W (eds)  
887 CMS books in mathematics/Ouvrages de Mathématiques de la SMC, 2nd edn. Springer, Cham

888 Zhao X-Q, Hutson V (1994) Permanence in Kolmogorov periodic predator-prey models with diffusion.  
889 *Nonlinear Anal* 23:651–668

890 **Publisher's Note** Springer Nature remains neutral with regard to jurisdictional claims in published maps  
891 and institutional affiliations.